9950-997

Picosecond Flash Spectroscopic Studies on Ultraviolet Stabilizers and Stabilized Polymers

Final Report

Jet Propulsion Laboratory Contract 955671

Contractor: University of California, Riverside

Principal Investigator: Gary W. Scott
Associate Professor of Chemistry

Date: 23 June 1982

This work was performed for the Jet Propulsion Laboratory, California Institute of Technology and was conducted pursuant to an Interagency Agreement between the Department of Energy (DOE) and the National Aeronautics and Space Administrative (NASA) and in furtherance of work under Prime Contract NAS7-100 between NASA and the California Institute of Technology.

(NASA-CR-169211) PICOSECOND FLASH SPECTROSCOPIC STUDIES ON ULTRAVIOLET STABILIZERS AND STABILIZED POLYMERS Final Report (California Univ.) 46 p
HC A03/MF A01

N82-30399

CSCL 07C G3/27

Unclas
28599

Technical Content Statement

This document contains information prepared by the University of California, Riverside, under JPL sub-contract. Its content is not necessarily endorsed by the Jet Propulsion Laboratory, California Institute of Technology, or its sponsors.

Abstract and Summary

Spectroscopic and excited state decay kinetics are reported for monomeric and polymeric forms of ultraviolet stabilizers in the 2-(2'-hydroxyphenyl)-benzotriazole and 2-hydroxybenzophenone classes. For some of these molecules in various solvents at room temperature, we report the following: (1) ground state absorption spectra, (2) emission spectra, (3) picosecond-time-resolved transient absorption spectra, (4) ground state absorption recovery kinetics, (5) emission kinetics, and (6) transient absorption kinetics. In the solid state at low temperatures ($T \gtrsim 12K$) we report emission spectra and their temperature-dependent kinetics up to $\sim$200K as well as, in one case, the 12K excitation spectra of the observed dual emission.

Three publications have originated directly from UCR, based on this work. In addition, two publications originating from JPL have included the results of this study and additional papers are in preparation.

A model which rationalizes the experimental findings for the 2-(2'-hydroxyphenyl) benzotriazole class of photostabilizers was presented in the recent UCR publications. This model includes efficient tautomerization in the excited state to a proton-transferred form, rapid internal conversion in room temperature solution before vibrational relaxation, and the possibility of measuring the barrier to proton transfer in low temperature solids. Internal conversion of the tautomeric form of the molecule is believed to be promoted by an internal rotational (or librational) mode of the molecule which includes relative rotation of the two ends of the molecule.

1. Published Reports

The major findings of this project have recently been reported in two papers:

(I) A. L. Huston, G. W. Scott, and A. Gupta, "Mechanism and Kinetics of Excited-State Relaxation in Internally Hydrogen-Bonded Molecules: 2-(2'-hydroxy-5'-methylphenyl)-benzotriazole in Solution," J. Chem. Phys., 76, 4978 (1982).

(II) A. L. Huston and G. W. Scott, "Picosecond Kinetics of Excited State Decay Processes in Internally Hydrogen-Bonded Polymer Photostabilizers," Proc. Soc. Photo-Opt.

Instrum. Eng. 322, 215 (1981).

Copies of these 2 papers are attached to this report as Appendices (I) and (II), respectively. In addition, an earlier paper contained some of the preliminary results of this project:

(III) A. L. Huston, C. D. Merritt, G. W. Scott, and A. Gupta, "Excited State Absorption Spectra and Decay Mechanisms in Organic Photostabilizers," in Picosecond Phenomena II, Springer Series in Chemical Physics, 14, 232 (1980).
This paper in included as Appendix (III).

Paper (I) includes and interprets the major findings on the 2-(2'-hydroxy-5' methylphenyl)-benzotriazole (Tinuvin P) photostabilizer in room temperature solution. It includes the measurements of ground state absorption recovery kinetics, fluorescence spectra and kinetics and solvent and deuteration effects in room temperature solution. A model involving excited state proton transfer is presented for the decay mechanism, rationalizing the known experimental data.

Paper (II) includes additional room temperature data on Tinuvin P as well as low temperature emission spectra and kinetics on this molecule. In addition, room temperature kinetics data are also presented for 2-(2'-hydroxy-3',5'-ditert-amylphenyl)-benzotriazole (Tinuvin 328) and the copolymer of 2-(2'-hydroxy-5'-vinylphenyl)benzotriazole with methyl methacrylate. Again a mechanistic model is presented which rationalizes both the low temperature and room temperature data obtained during this project.

Paper (III) contains the room temperature transient absorption spectra of the above-mentioned molecules as well as of 2-hydroxybenzophenone and a copolymer of this molecule. The results presented in that paper were preliminary, as was the model, and the results and conclusions in papers (I) and (II) supercede the interpretations included in paper (III).

2. Additional Results.

Some of the data obtained during the course of this project have not yet been included in any publications. These results, and tentative interpretations of them,

are discussed below.

2.1. Room Temperature Absorption Spectra

A room temperature UV-VIS absorption spectrum between 250 and 400 nm of Tinuvin P was taken in trifluoroethanol (CF_3CH_2OH) and is shown in Fig. 1. For comparison, a spectrum of Tinuvin P in ethanol is shown in the same figure. The absolute absorbance intensities are not significant. Note the change in the relative intensities in the two absorption peaks. Also, there is a blue shift of ∿10 nm for the trifluoroethanol solvent as opposed to ethanol. An absorption spectrum for Tinuvin P in methylcyclohexane is shown in Fig. 2. A blue shift of ∿15 nm is observed for the trifluoroethanol solvent relative to methylcyclohexane.

The extinction coefficient for Tinuvin P in ethanol at 355 nm is $\sim 1 \times 10^4$ indicating that absorption is probably due to a $\pi\pi^*$ transition. The blue shift in the more strongly hydrogen bonding solvents suggests that the ground state of Tinuvin P is stabilized through hydrogen bonding with the solvent. This ground state stabilization may be important in the kinetics of proton transfer. We report below increased excited lifetimes in polar, hydrogen bonding solvents.

2.2. Low Temperature Absorption Spectra

Low temperature absorption spectra were obtained for Tinuvin P in two glasses at T=10 K. Figure 3 shows the absorption spectrum in methylcyclohexane; Figure 4 shows the spectrum in EPA (diethylether, isopentane and ethyl alcohol, 5:5:2). A number of interesting features arise on going to low temperature. First of all, a prominent shoulder appears on the red edge of the absorption band at approximately 370 nm. A very weak band also appears at ∿385 nm. The peak centered at 340 nm in the room temperature spectrum is resolved into a doublet at low temperature. In methylcyclohexane the doublet peaks occur at 350 and 340 nm while in EPA the peaks are at ∿347 and 336 nm. The relative intensities of the doublet peaks are different for the hydrogen-bonding EPA solvent compared to methylcyclohexane as solvent. This suggests that the doublet may be the result of different hydrogen bonded conformations in the two glasses.

Figure 1: Room Temperature Absorption Spectra

—— Tinuvin P / CF_3CH_2OH

---- Tinuvin P / CH_3CH_2OH

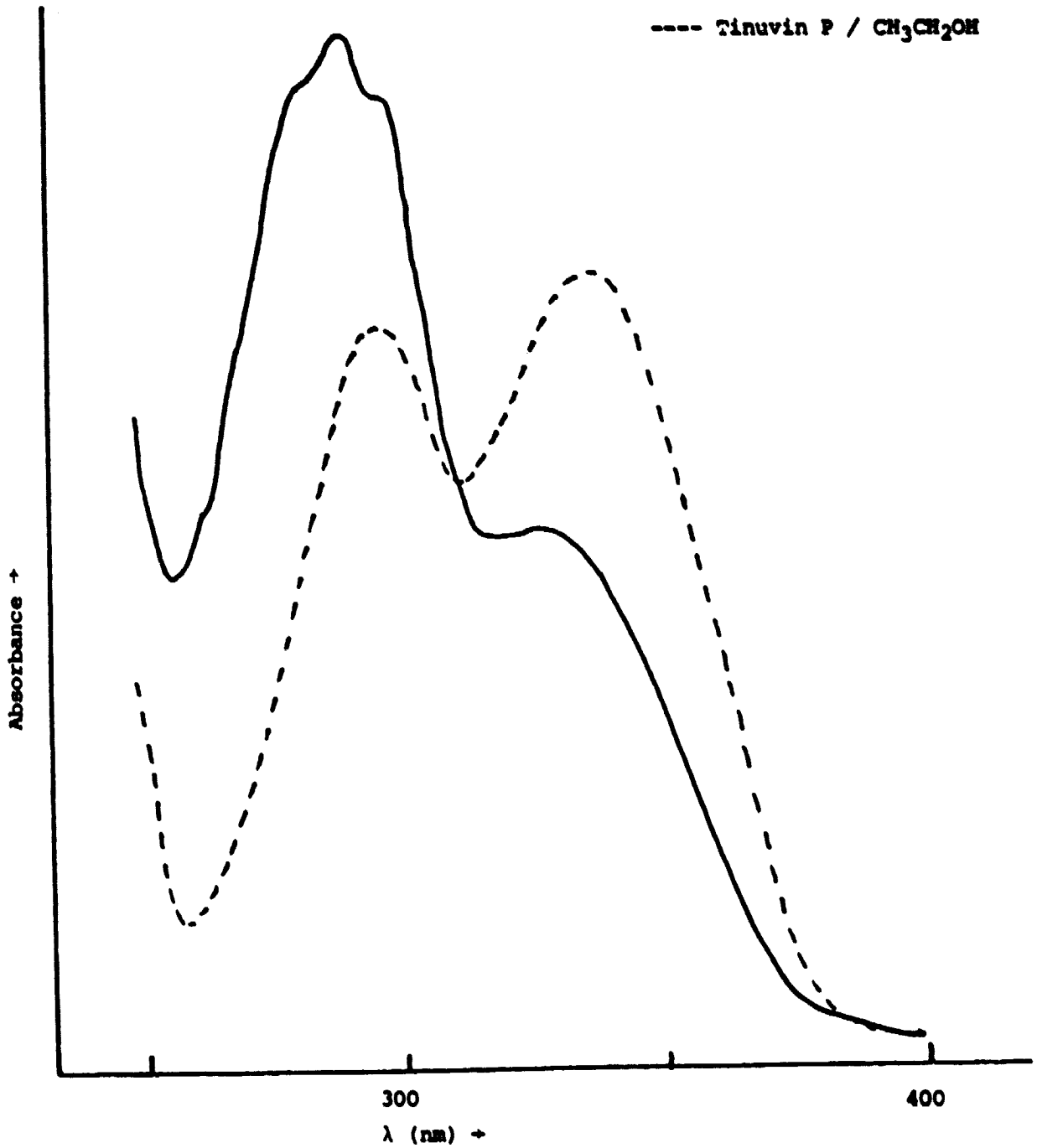

Figure 2: Room Temperature Absorption Spectra

Tinuvin P / Methylcyclohexa

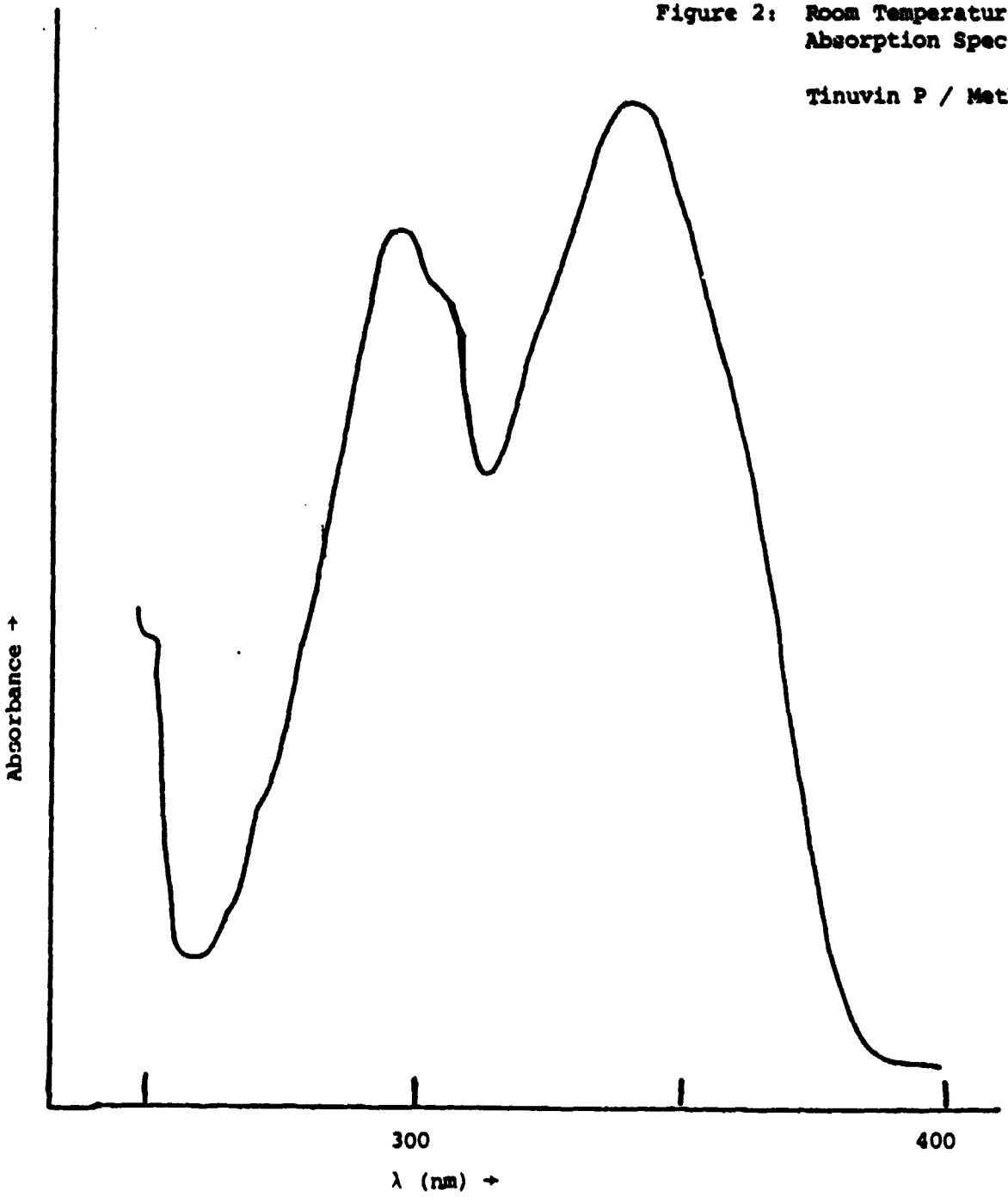

Figure 3: 10 K Absorption Spectrum

Tinuvin P / Methylcyclohexane

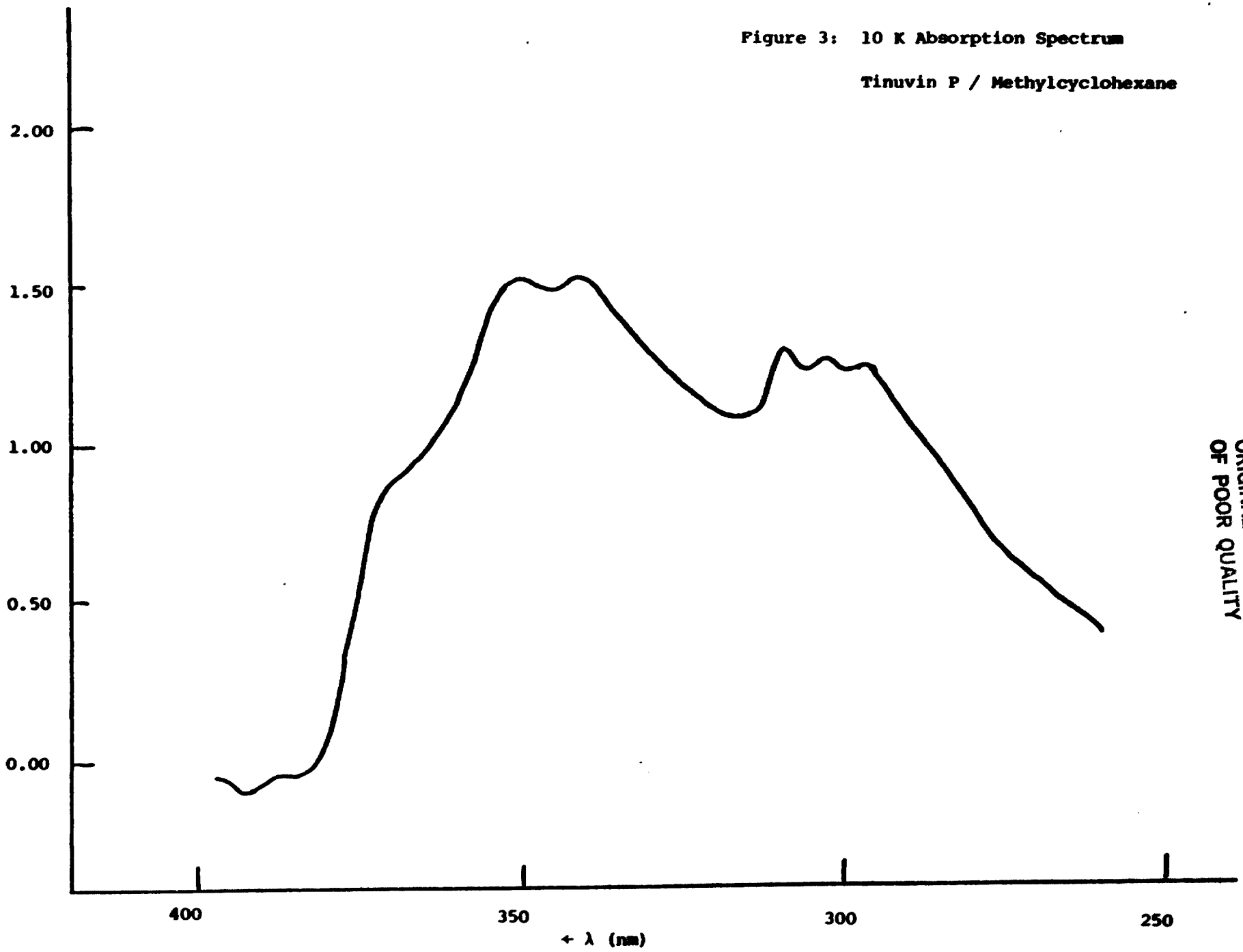

ORIGINAL PAGE IS
OF POOR QUALITY

Figure 4: 10 K Absorption Spectrum

Tinuvin P / EPA

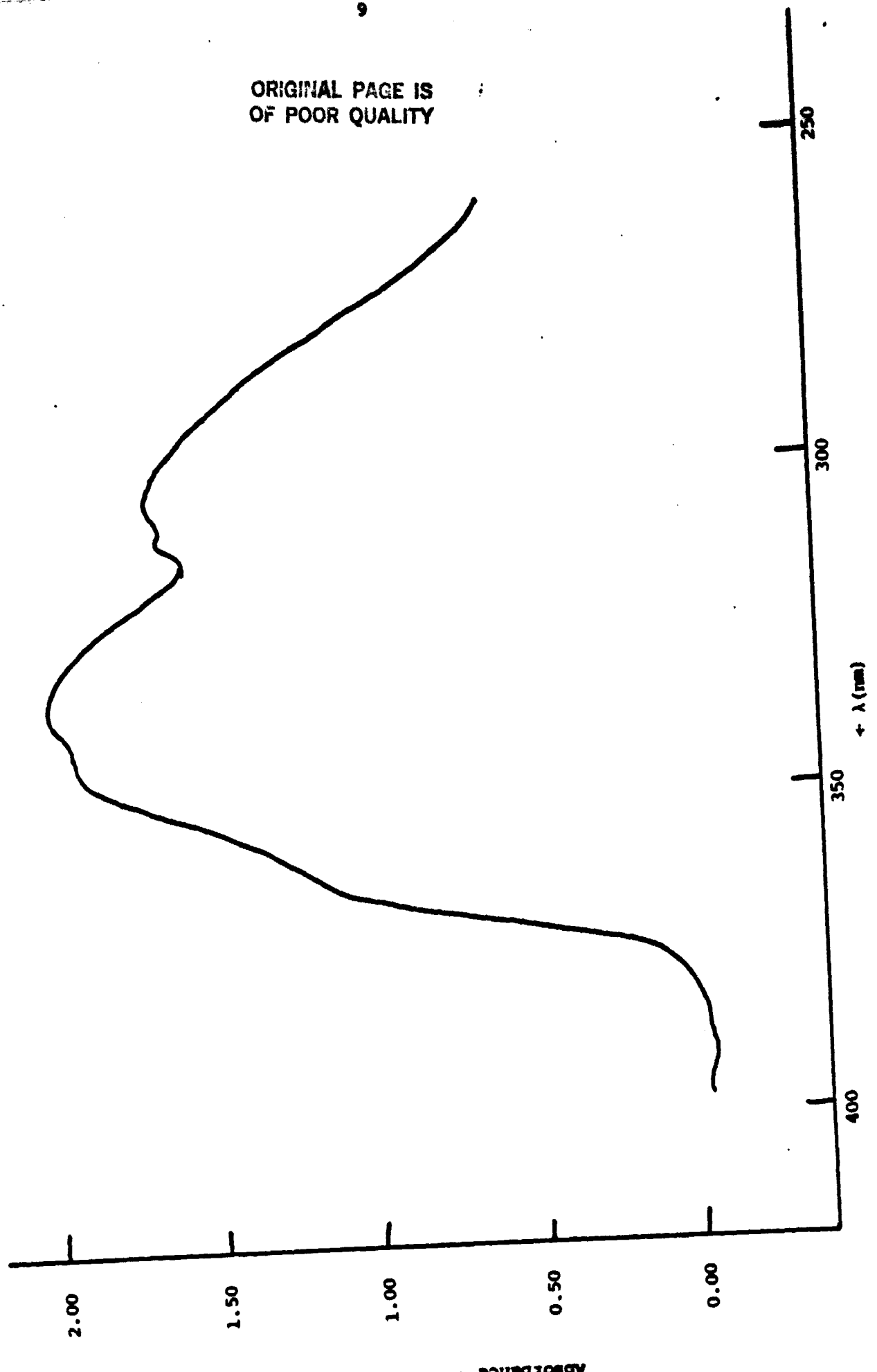

The band centered at approximately 300 nm at room temperature also shows the appearance of structure on going to low temperature. The structure is more pronounced in methylcyclohexane than in EPA. This band appears to be made up of a triplet of peaks in methylcyclohexane but is not resolved in EPA. In contrast to the peaks at ~340-350 nm, the 300 nm peak does not shift significantly with solvent.

2.3. Low Temperature Emission Spectra

2.3.1. Intensity Dependence in n-octane Glass

Low temperature emission spectra of Tinuvin P in n-octane were obtained showing red fluorescence with λ_{max} = 625 nm and fluorescent intensities which are strongly temperature dependent. The fluorescence spectrum of Tinuvin P at 11 K, corrected for the spectral response of the detector, is shown in Figure 5. Figure 6 shows the fluorescence intensity dependence on temperature (not corrected for spectral response.) Variation of this intensity with temperature presumably is due to the decrease in excited-state lifetime as the temperature is increased. This variation is documented in Appendix (II). The red emission observed at 11 K is essentially identical to that observed by Werner at 90 K in a hydrocarbon glass. Red fluorescence could be seen to begin just as the solvent began to form a rigid glass, the intensity increasing as the temperature decreased. No shift was observed in the position of the fluorescence maximum.

Sample excitation was accomplished using the 325 nm line of a HeCd laser. Fluorescence was collected and analyzed with a one meter Hilger Engis scanning monochromator/spectrograph equipped with an S-20 photomultiplier tube. Samples were cooled in a closed cycle helium refrigerator. Fluorescence intensity measurements were carried out by first cooling the sample to its lowest temperature, 11 K, then taking spectra as the temperature was stepped up. This technique was used to avoid changes in intensity due to changes in the degree of cracking in the glass. (n-octane forms a very opaque glass, the physical appearance of the glass was not observed to change over the temperature range studied.)

Figure 5: 11 K Emission Spectrum

Tinuvin P / n-octane

(Corrected for spectral response)

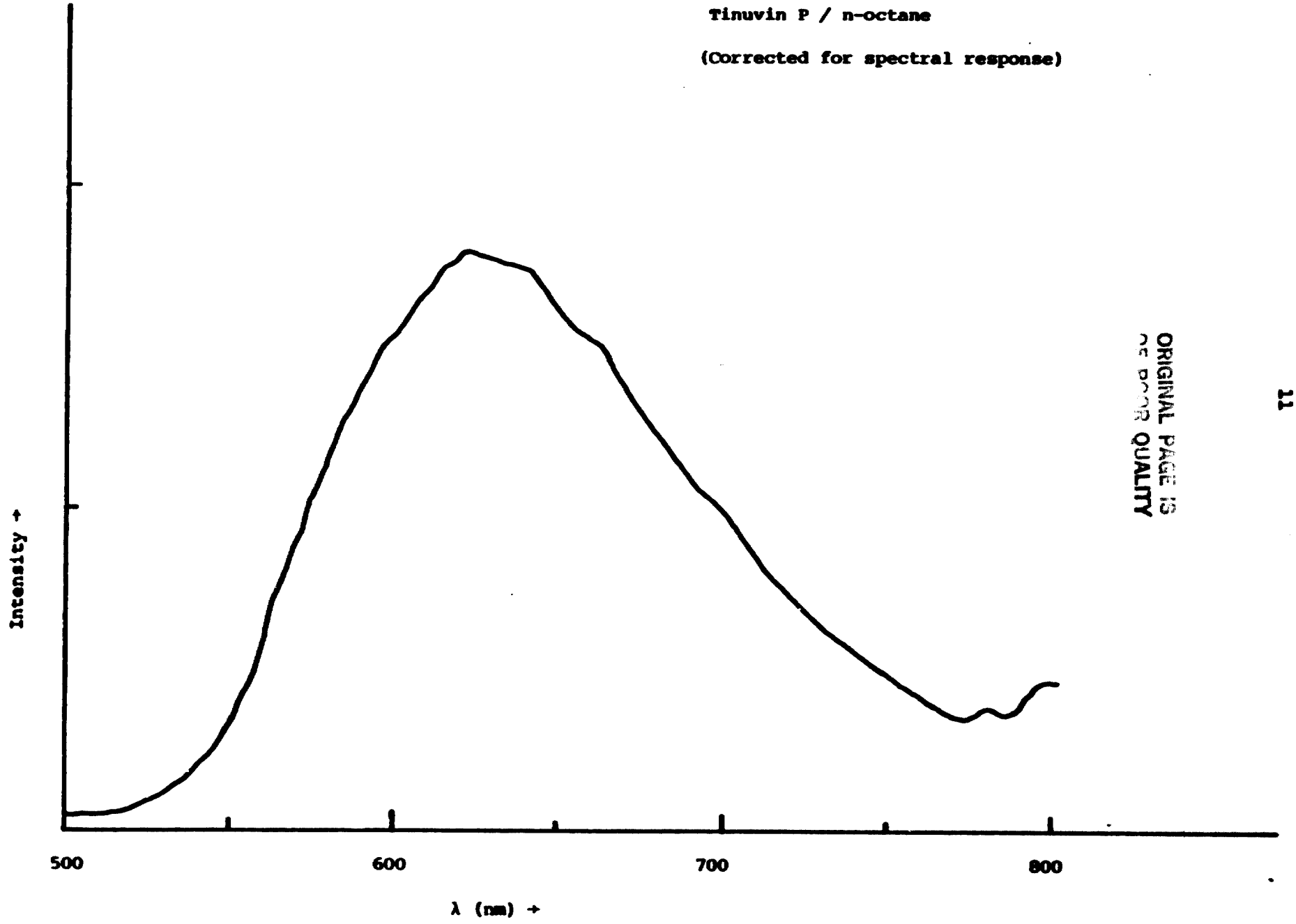

Figure 6: Fluorescence of Tinuvin P / n-octane at Different Temperatures

(Not corrected for spectral response)

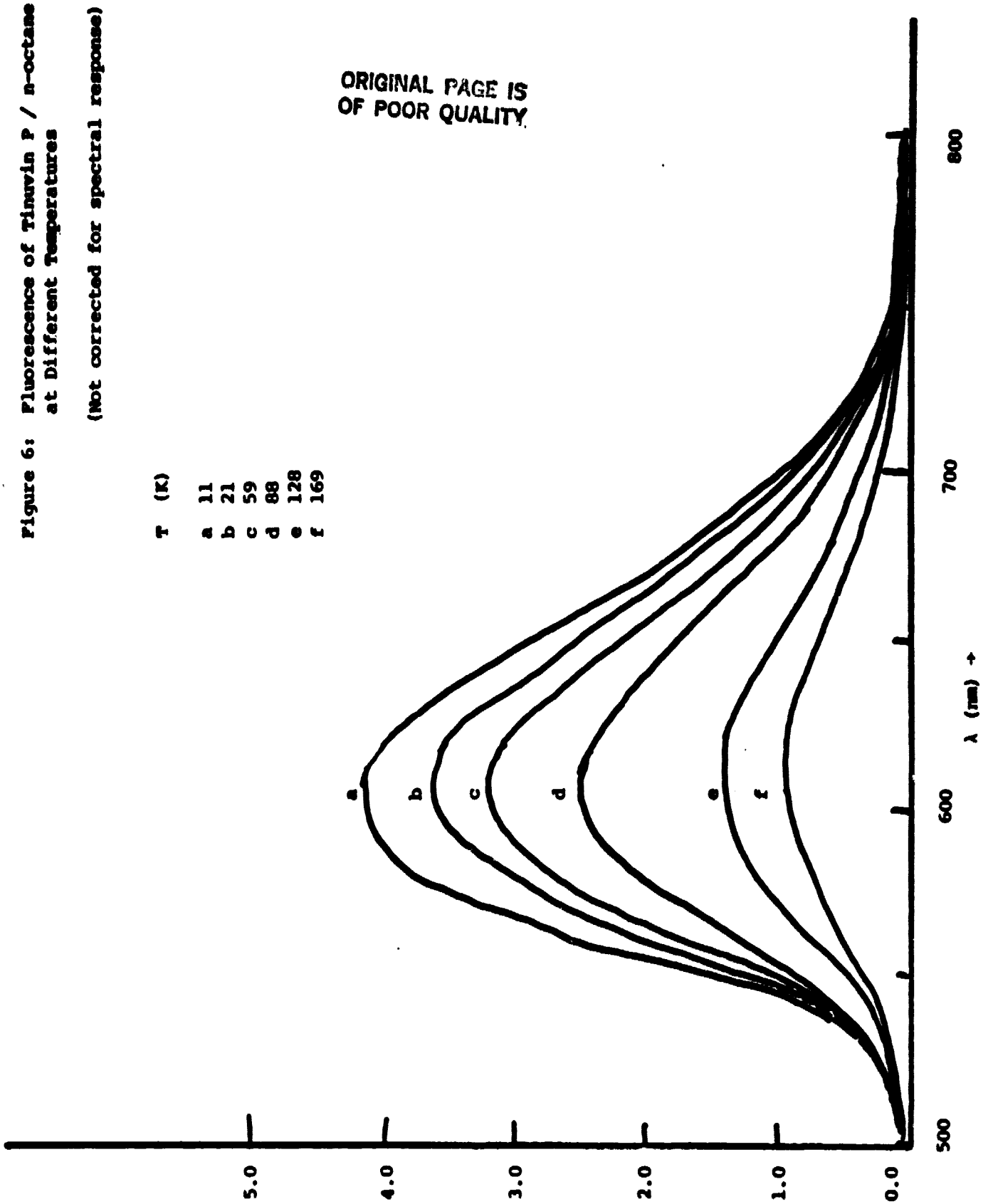

2.3.2. Fluorescence at 4.2 K in Pure Crystal

Continuously excited emission spectra of Tinuvin P crystals at 4.2 K were obtained. Fig. 7 shows the spectrum resulting from 325 nm excitation using a Helium-Cadmium laser. Fig. 8 shows the spectrum obtained exciting with 365 nm line from a high-pressure mercury lamp. The two spectra appear identical, suggesting that there is no excitation wavelength dependence of the red emission in that region. A small amount of structure appears on the blue edge of the emission band. The bands are indicated by letters a, b and c and have the following spacings:

a - b	515.8 ± 10.1 cm^{-1}
a - c	870.2 ± 23.6 cm^{-1}
b - c	354.3 ± 18.1 cm^{-1}

The a, b and c peaks occur at 543 nm, 558 nm and 570 nm, respectively.

2.3.3. Low Temperature Fluorescence Decay Kinetics

Temperature-dependent, fluorescence decay kinetics were obtained for Tinuvin P in a hydrocarbon glass (n-nonane) and these results are discussed in Appendix II. In addition, fluorescene decay kinetics were obtained for Tinuvin P in ethanol at 12 Kelvin. Immediately after cooling the sample to 12K, two distinct fluorescence maxima were observed in this solvent, one having λ_{max} ~400 nm, the other at λ_{max} ~600 nm. These fluorescence decay experiments were performed using a 355 nm, 10 picosecond pulse from a Nd^{3+}:glass laser. Emission wavelengths were isolated using appropriate combinations of color glass filters. A band consisting of wavelengths between ~400 nm and 480 nm was isolated using a Schott BG3x2 and a GG400x3. Red emission (λ_{fl} > 550 nm) was isolated using a OG550x3 filter. The two emissions exhibited different lifetimes--τ_{400} ~2ns, τ_{600} ~1ns. After the sample had been maintained at 12K for several hours, the red emission was no longer detectable.

The observation of two emission maxima with different lifetimes indicates the existance of two distinct species or forms of Tinuvin P in the ethanol matrix. The disappearance of the red component after several hours at 12K suggests that some

Fig. 7. Emission from Tinuvin P at 4.2 Kelvin using 325 nm excitation. Tics at 550 nm and 600 nm are wavelength markers. Spectrum not corrected for instrument response.

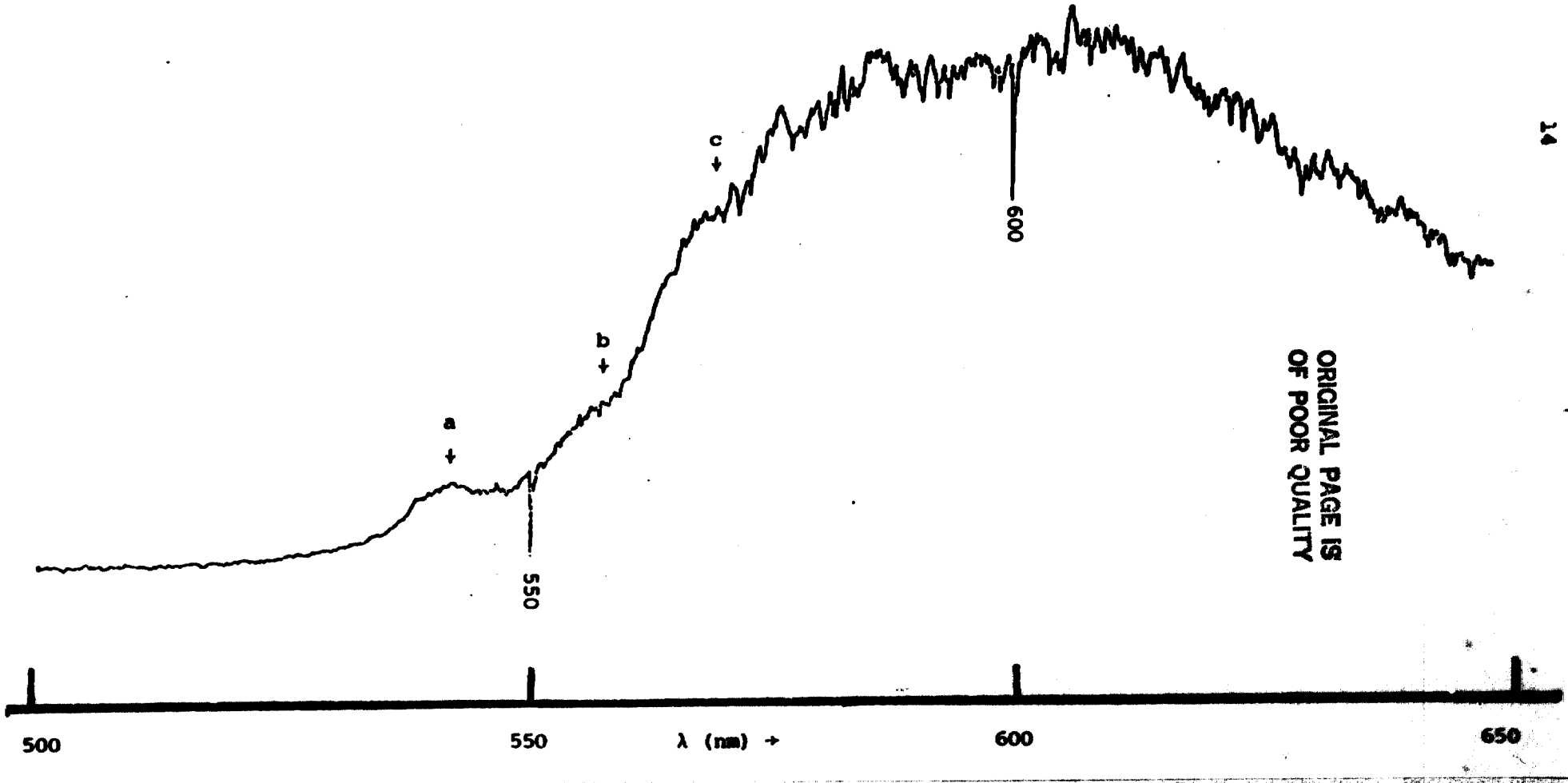

Fig. 8. Emission from Tinuvin P crystal at 4.2 Kelvin using 365 nm excitation. Tics at 530 nm, 586 nm and 610 nm are wavelength markers. Spectrum not corrected for instrument response.

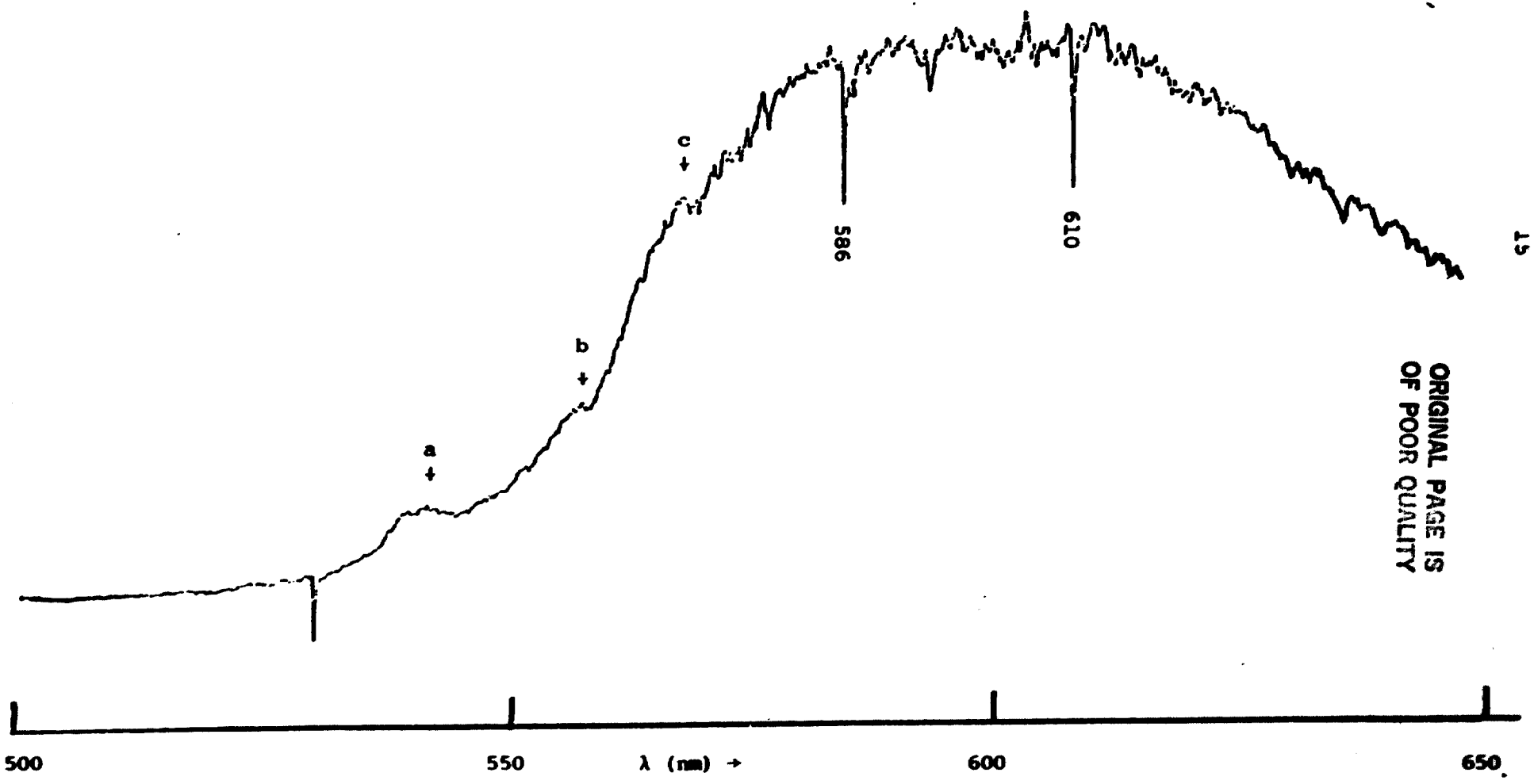

ground state equilibration process is occurring. A reasonable explanation of the data is that upon cooling, some of the Tinuvin P molecules are initially frozen in a conformation which is intramolecularly hydrogen bonded This conformation could be responsible for highly Stokes-shifted red emission which arises due to excited state intramolecular proton transfer. The blue emission may be due to intermolecularly hydrogen bonded molecules. The preference for intermolecularly hydrogen bonded molecules is probably due to a greater decrease in free energy resulting from the formation of as many as three intermolecular hydrogen bonds with the solvent. The loss of red emission over a period of several hours at low temperature is due to slow reorientation and equilibration of the Tinuvin P molecules to give the energetically favored intermolecularly hydrogen bonded species.

2.4. Low Temperature Fluorescence Excitation Spectra

The fluorescence excitation spectrum of Tinuvin P in methylcyclohexane at 12 Kelvin has been obtained in the wavelength region 370-390 nm. Two excitation spectra were obtained, one monitoring emission at 600 nm, the other monitoring at 420 nm. The spectra are shown in Figure 9. The two spectra differ significantly in the relative intensity ratios of 370 nm to 385 nm excited emission. The ratio of the red fluorescence intensity excited at 370 nm and 385 nm is approximately 0.8 whereas the ratio of the blue intensity excited at the same wavelength is ∿.25. The absorption spectrum of Tinuvin P (Figure 3) has a weak band on the red edge which corresponds to the peak at 385 nm in the excitation spectrum. Emission from this state is approximately one to one blue vs. red emission. Higher energy excitation results in primarily red emission.

The experiments were conducted using a nitrogen laser pumped dye laser operating at 10 Hz. Exciton BPBD-365 laser dye was used to cover the wavelength range 365-395 nm.

Figure 9: Fluorescence Excitation Spectrum of Tinuvin P / Methylcyclohexane.

(Detection at wavelengths indicated)

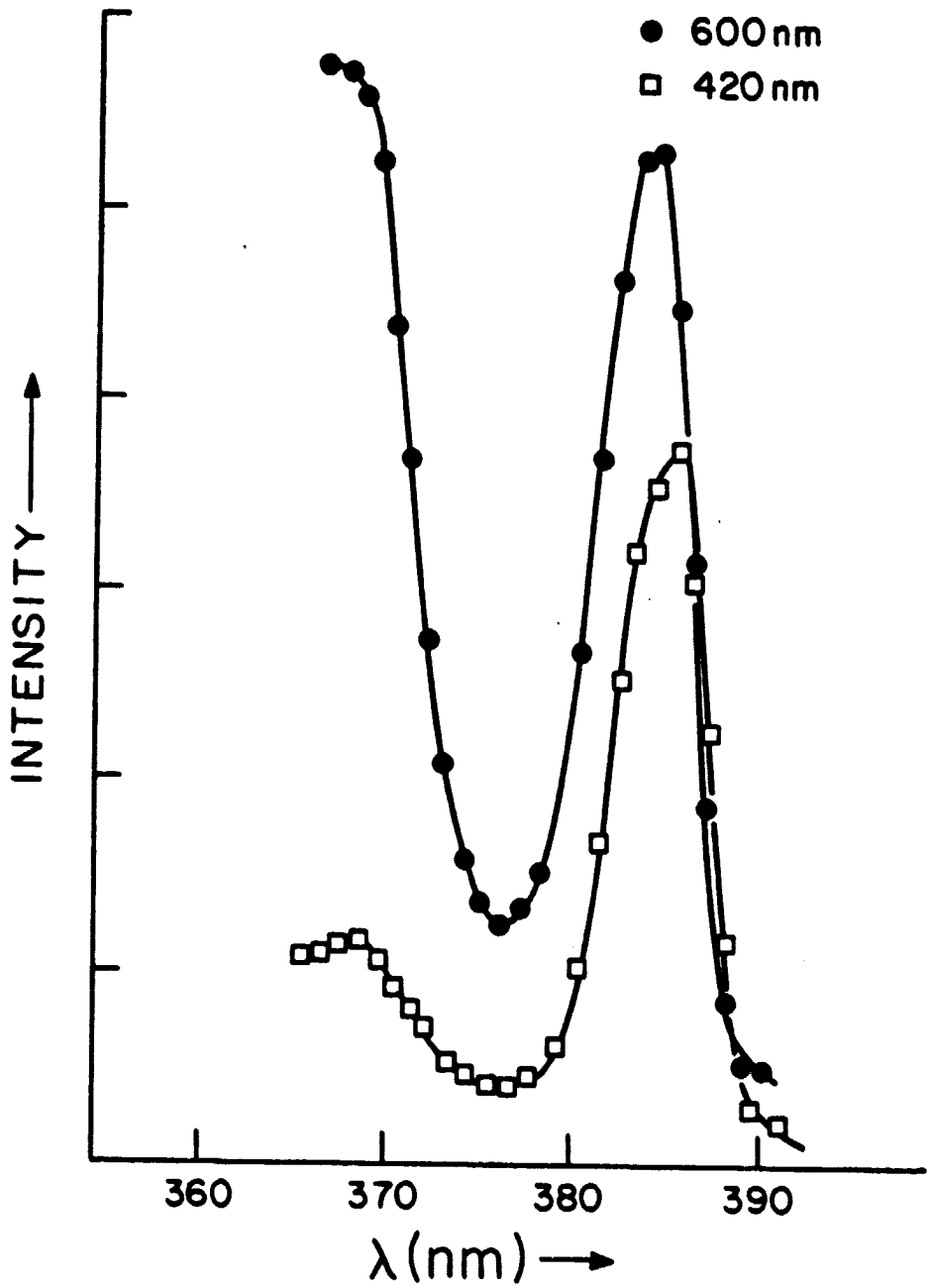

3. Summary of Experimental Results:

Comprehensive summaries of the experimental results obtained during this study are presented in Tables I, II and III. The combination of experimental techniques employed has enabled us to propose a concise model describing the photophysical behavior of orthohydroxyphenylbenzotriazoles following ultraviolet excitation. The following section, Mechanistic Interpretation, is a compilation of the discussions presented in the two most recent publications: A. L. Huston, G. W. Scott and A. Gupta, J. Chem. Phys. 76 (10), 4978 (1982) and A. L. Huston and G. W. Scott, Proc. Soc. Photo-Optic. Instrum. Engin. 322, 215 (1982).

Table I. Summary of room temperature excited state kinetics of substituted hydroxyphenylbenzotriazoles.

Molecule	Solvent	Absorption Recovery τ(ps) at 355 nm	Fluorescence Decay τ(ps)
2-(2'-hydroxy-5'-methylphenyl) benzotriazole (Tinuvin P)			
Tinuvin P	Methylcyclohexane	33±5	14.4±3.4
Tinuvin P-d_1	Methylcyclohexane	22±5	---
Tinuvin P	Ethanol	74±10	52.0±3.8
Tinuvin P	Methylene Chloride	29±5	19.1±4.8
Tinuvin P	Hexadecane	33±3	---
2-(2'-hydroxy-3',5'-di-tert-amylphenyl) benzotriazole (Tinuvin 328)	Methylcyclohexane	40±15	---
2-(2'hydroxy-5'-vinyl-phenyl) benzotriazole: MMA copolymer	Methylene Chloride	25±5	15±4

Table II. Low Temperature Kinetics of Tinuvin P and Tinuvin P-d_1 in n-nonane at 12K.

Molecule	Fluorescence Decay τ (ns)	Activation Energy (cm^{-1})
Tinuvin P	0.82±.07	282±43
Tinuvin P-d_1	1.20±.10	193±33

Table III. Low Temperature Emission Spectra of Tinuvin P at 11K.

Solvent	λ_{max} Fluorescence (nm)	λ_{max} Phosphorescence (nm)
n-octane	∿625	---
ethanol	∿400	475, 529, 545

4. Mechanistic Interpretation

Considering the experimental data presented above, we propose a model for excited state deactivation of Tinuvin P which is a slightly modified version of the model proposed earlier by Otterstedt and Werner. The overall mechanism that they proposed may be written as follows:

$$S_0 \xrightarrow{h\nu} S_1 \xrightarrow[\text{transfer}]{H^+} S_1' \xrightarrow{ic} S_0' \xrightarrow[\text{transfer}]{H^+} S_0 \qquad (1)$$

The major steps in the mechanism following absorption of the uv light are first of all proton transfer to give the zwitterionic form, S_1', followed by rapid internal conversion to give the proton transferred ground state form S_0' which then rapidly equilibrates to give the ground state form, S_0. The new kinetic and spectroscopic evidence that we presented above allows us to provide a more detailed account of the mechanism. The basic processes involved are shown schematically in Figure 10.

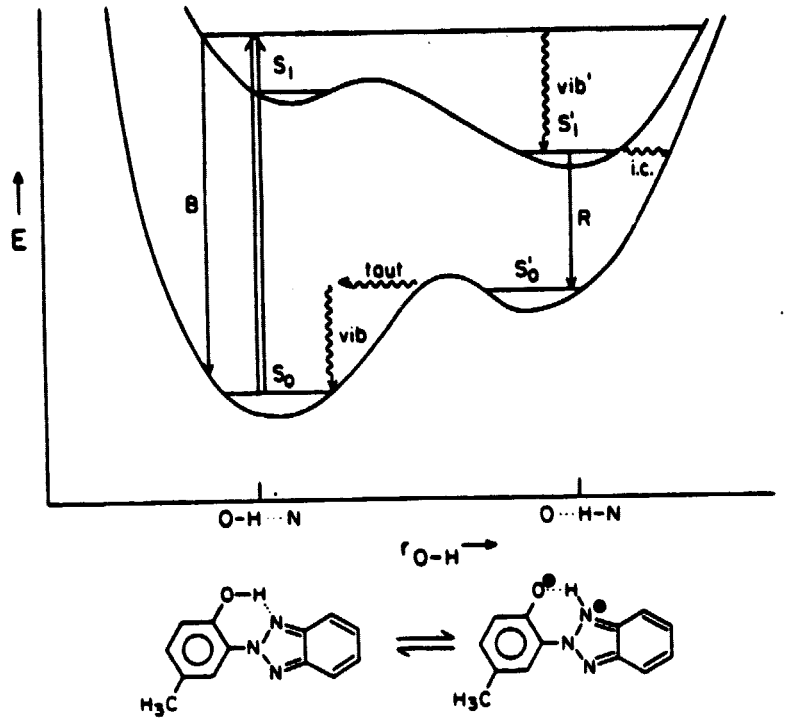

Figure 10. Potential energy surfaces and details of the absorption and excited state deactivation processes in Tinuvin P.

Based on the absorption spectrum of Tinuvin P in aprotic solvents, compared to its spectrum in the strongly hydrogen-bond-breaking trifluoroethanol solvent, we assert that the absorption band at 350 nm is primarily due to the intramolecularly hydrogen-bonded form of Tinuvin P. Absorption at 355 nm produces an excited vibrational level in S_1. Room temperature fluorescence spectra and kinetics in hydrocarbon solution exhibit blue emission (B), λ_{max} ~410 nm, $\tau \sim 14$ ps with an estimated quantum yield of $2\text{-}5 \times 10^{-5}$. Ground state recovery kinetics measure the rate of the overall process to be ~30 ps in hydrocarbons. We propose that the room temperature emission be identified as fluorescence from a vibrationally unrelaxed S_1 state (B in Fig. 10). This assignment is not unreasonable since the fluorescent lifetime (14 ps) is within the range of excited state vibrational relaxation times reported for other large aromatic molecules. Excitation to a vibrationally "hot" level in S_1 may lead to the establishment of an equilibrium between S_1 and the proton transferred form S_1'

prior to vibrational relaxation. The fluorescence decay time would then be determined by the rate of internal conversion, $S_1' \rightsquigarrow S_0'$. If this is the case, the mechanism shown above (eqn. (1)) should be modified to show an equilibrium between S_1 and S_1' and that internal conversion $S_1' \rightsquigarrow S_0'$ occurs prior to vibrational relaxation:

$$S_0 \xrightarrow{h\nu} S_1 \underset{H^+}{\overset{K}{\rightleftharpoons}} S_1' \xrightarrow{ic} S_0' \xrightarrow{H^+} S_0. \qquad (2)$$

The observation of longer fluorescence and ground state recovery lifetimes in ethanol suggests that intermolecular hydrogen bonds with the solvent may inhibit the excited state proton transfer process and/or shift this equilibrium.

Low temperature fluorescence studies in hydrocarbon matrices show an emission maximum at ∿625 nm, and lifetimes of ∿1 ns at 12K. This emission (R) is assigned to the transition $S_1' \longrightarrow S_0'$ of the proton transferred species shown in Figure 10. The temperature dependence of the fluorescence lifetime is assumed to be wholly due to a temperature dependent nonradiative rate. The activation energy for the temperature dependent nonradiative decay, ∿200 cm^{-1}, is of the order of magnitude expected for a torsional vibrational mode. This mode would be expected to be an important factor in the rapid rate of internal conversion in Tinuvin P.

In the ethanol glass at 12K no highly Stokes shifted emission was observed. The fluorescence maximum occurs at 410 nm, the same region as in the room temperature emission, and in addition, green phosphorescence is observed at 12K. It appears then that in the low temperature ethanol glass, intramolecular ptoron transfer is slowed and/or the equilibrium shifted to the left in Figure 10, and intersystem crossing becomes a competing conradiative decay route.

With reference to Figure 10, then, the predominant decay route in the proposed model for relaxation of Tinuvin P involves uv excitation (double upward arrow) into an excited vibronic level of the molecule that lies at an energy (for 355 nm

data sets are shown in Figs. 4(B) and 4(C), respectively.] The lifetime values obtained in these two fits are reported in Table I. The error estimates for these values were obtained by assuming the uncertainty in the position of $t=0$ was ±4 channels (see Sec. IIC) of the OMA (~±2.5 ps), thereby obtaining the range of lifetimes reflected by the error estimates given in Table I. These error estimates were always larger (by ~5×) than the standard deviation in the lifetime parameter obtained in the minimum rms (best) fit. (This same procedure was also applied to each single-laser-shot-produced, ethanol solvent data set, and resulted in error estimates, which were approximately the same as the standard deviation in the average reported in Table I. It should be noted that the "best" fits obtained for each single-laser-shot data set established the position of $t=0$ relative to the etalon marker pulse to within ±2 channels from data set to data set.)

In Fig. 4 and for the fluorescent lifetimes given in Table I, the only wavelength discrimination of the fluorescence was provided by a UV blocking filter (Schott, GG 400) to isolate the fluorescence from the laser pulse. For (I) in ethanol only, the short-lived emission was strong enough to allow the use of narrower bandwidth filters to determine the wavelength range of the fluorescence. For example, allowing only emission wavelengths in the range 400 nm $\lesssim\lambda\lesssim$ 460 nm (Schott GG 400×3 mm, Schott BG 14×3 mm, and Ditric 4600 short-pass cut-off filters), essentially identical emission kinetics were observed for (I) in ethanol as those given in Fig. 4 and Table I. (The best-fit lifetimes for averaged data from three laser shots was in this case 50.1 ps with an error estimate of ±7.8 ps.) On the other hand, for the same sample, blocking all emission wavelengths shorter than ~570 nm (Schott OG 570×3 mm) resulted in a streaked fluorescence signal only barely discernible above background; i.e., less than a few percent of the total short-lived detected visible fluorescence was in a wavelength region to the red of 570 nm. Steady-state emission spectra indicate that fluorescence maxima of (I) in all solvents at room temperature occurs at $\lambda_{max}\lesssim 410$ nm. (See below.)

The short-lived fluorescence kinetics of (I) in ethanol were found to follow an exponential decay, within experimental error, as shown in Fig. 5. The short-lived fluorescence kinetics in methylcyclohexane and methylene chloride were too weak to allow for exact determination of the form of the decay, but were assumed to also be exponential in the fitting procedure.

Broad, featureless emission spectra were observed for (I) in methylene chloride, ethanol, methylcyclohexane, and cyclohexane solvents at room temperature. Initial experiments with the commercial spectrofluorimeter on (I) in the methylene chloride and ethanol solvents indicated very weak emission with maxima in the blue and fluorescence quantum yields on the order of $\sim 2\times10^{-5}$. Subsequently, quantum yield estimates were made using the high sensitivity spectrofluorimeter[28] on (I) in cyclohexane. In this case the emission maximum was at $\lambda_{max}\sim 410$ nm, and the fluorescence quantum yield was estimated to be in the range 2×10^{-6} to 5×10^{-6}. Finally, emission spectra of (I) were obtained with the laser Raman spectrometer (see Sec. IID) in the solvents cyclohexane, methylcyclohexane and ethanol. In every case, the emission maximum occurred in the range $\lambda_{max}\sim 405$–410 nm and the emission intensities were similar. No emission intensity was observed to the red of ~500 nm.

IV. DISCUSSION

A. Excited-state kinetics

The kinetics data presented above provide new information concerning the excited-state decay mechanism of (I). In the first place, in three solvents, the fluorescence decay of (I) was found to occur faster than did the ground-state absorption recovery of (I) at 355 nm. This observation suggests a mechanism involving sequential decay of the fluorescent state through other intermediate state(s) and/or tautomeric form(s) before ground-state recovery is complete. This model might require that the ground-state recovery be somewhat nonexponential but deviations from nonexponential behavior need not be too severe and could easily be masked by the signal-to-noise evidenced by the experimental data (Figs. 2 and 3). From the present ground-state absorption recovery experiments on (I), it is clear that no significant quantum yield of long-lived species is obtained. These results indicate that the major decay pathway involves only singlet species of the molecule.

Another important feature of our results is that both the fluorescence decay and the ground-state absorption recovery lifetimes of (I) are longer in the intermolecular hydrogen bonding solvent (ethanol) than in the non-hydrogen bonding solvents. This observation suggests that the ethanol solvent may competitively form *intermolecular* hydrogen bonds with (I), disrupting the intramolecular hydrogen bond and slowing the excited-state relaxation process as suggested in Sec. I and in Fig. 1.

To investigate the possibility that the kinetics of radiationless deactivation of (I) is affected by solvent viscosity, the ground-state recovery kinetics of (I) was investigated in two different hydrocarbon solvents of different viscosity at room temperature: methylcyclohexane ($\eta=0.73$ cp) and hexadecane ($\eta=3.34$ cp). Viscosity-dependent nonradiative rate constants have been determined previously for a number of molecules containing internally rotating phenyl groups.[29–33] If *free* rotation about the C–N single bond joining the phenol and benzotriazole parts of (I) modified its radiationless decay rate in the same way[33] then the decay time observed in hexadecane would be expected to be ~50% longer than in methylcyclohexane. The lack of a viscosity effect on the nonradiative decay rate in (I) suggests that rotation about the C–N bond may be hindered, most likely due to the intramolecular hydrogen bond. In the case of a hindered rotor, it is not clear that the macroscopic viscosity of the solvent is the correct parameter to use in describing the microenvironment of the solute. However, emission studies, discussed below, indicate that the dihedral angle between the phenol

evidence for triplet formation in room temperature solutions of Tinuvin P in ethanol suggesting that internal conversion $S_1' \rightsquigarrow S_0'$ is very rapid compared to the rate of intersystem crossing.

Mechanism and kinetics of excited-state relaxation in internally hydrogen-bonded molecules: 2-(2′-hydroxy-5′-methylphenyl)-benzotriazole in solution[a)]

Alan L. Huston and Gary W. Scott

Department of Chemistry, University of California, Riverside, Riverside, California 92521

Amitava Gupta

Energy and Materials Research Section, Jet Propulsion Laboratory, California Institute of Technology, Pasadena, California 91103

(Received 9 July 1981; accepted 9 February 1982)

We report the ground state absorption recovery kinetics (at 355 nm) and the fluorescence spectra and kinetics of 2-(2′-hydroxy-5′-methylphenyl)-benzotriazole (I) following excitation at 355 nm in several solvents at room temperature. Measured lifetimes range from 14 to 75 ps. Fluorescence lifetimes are shorter than the corresponding ground state recovery times, indicating the intervention of intermediate forms during the excited state relaxation process. The measured fluorescence quantum yield is lower than one predicted by the usual calculated radiative rate for the near UV, strongly absorbing singlet state of this molecule. Decay rates are slower in ethanol than in nonhydrogen bonding solvents indicating that external interference with the intramolecular hydrogen bond in (I) slows the relaxation rate. The room temperature decay rates are not strongly affected by the solvent viscosity. Deuteration of the molecule produces only a slightly more rapid ground state recovery rate than in the protonated species. A model involving excited state proton transfer is presented for the decay mechanism, rationalizing the known experimental data.

I. INTRODUCTION

Intramolecular hydrogen bonds, present in a number of molecules containing phenolic hydroxyl groups and slightly basic carbonyl or amino groups, lead to a variety of interesting and unusual photophysical and photochemical properties.[1-21] Many of these molecules, such as derivatives of 2-hydroxybenzophenone and 2-(2′-hydroxyphenyl)-benzotriazole, are widely used as ultraviolet - absorbing polymer photostabilizers.[22,23] The intramolecular hydrogen bond in these molecules is thought to promote rapid, radiationless, excited-state decay. Large Stokes shifts observed in the emission spectra of many of these molecules suggest that excited-state proton transfer plays an important role in the excited-state relaxation mechanism. The mechanism and kinetics of these processes have yet, in many cases, to be determined. Related kinetics studies include work on salicylates,[7-9] salicylanilides,[10] 2-(2′-hydroxyphenyl-s-triazines,[6] 2-hydroxybenzophenones,[11-16] and 2-(2′-hydroxyphenyl)-benzotriazoles.[14,15,19]

In the present paper, we present new kinetic and spectroscopic studies of the mechanism of excited-state decay for 2-(2′-hydroxy-5′-methylphenyl)-benzotriazole (I) in room temperature solution. The ground-state structure of (I) in aprotic solvents and one possible tautomeric form (I′) resulting from ultraviolet excitation of (I) are shown in Fig. 1. Also shown in Fig. 1 is a possible ground state structure (II) for this molecule in an alcoholic solvent. The intermolecular hydrogen bonds illustrated by structure (II) could prevent or partially interfere with the formation of the intramolecular hydrogen bond which promotes the process (I) − (I′). The present investigation explores the mechanism and kinetics of the processes of ultraviolet excitation and excited state decay (I) ⇌ (I′) as well as the importance of structures like (II) in protic solvents. These studies include measurements of ground-state absorption bleaching and recovery kinetics, as well as excited-state fluorescence kinetics of (I) in both protic and aprotic solvents at room temperature. Also, determinations of room temperature fluorescence spectra and quantum yields are reported. An analysis of the results produced by these techniques gives rates of ex-

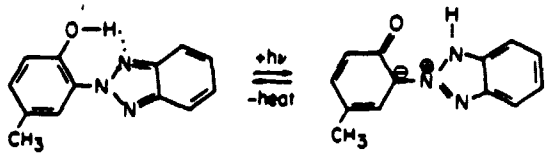

(I) (I′)

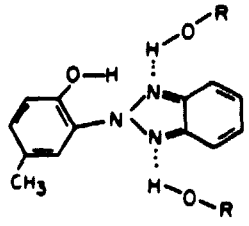

(II)

FIG. 1. Ground-state (I) and excited-state (I′) molecular structures of 2-(2′-hydroxy-5′-methylphenyl)-benzotriazole in aprotic solvents. Also shown is a possible structure (II) in alcoholic solvent.

a)This research was supported by the Polymer RAD task of the Solar Thermal Power Systems Project of the Jet Propulsion Laboratory, the University of California Appropriate Technology Program, and the Committee on Research at the University of California, Riverside.

 0021-9606/82/104978-08$02.10

cited-state relaxation processes, as well as a mechanism of the excited-state decay in this molecule.

II. EXPERIMENTAL TECHNIQUES

A. Samples

Commercially available 2-(2'-hydroxy-5'-methylphenyl)-benzotriazole (Tinuvin P, Ciba-Geigy) was purified by zone refining for 100 zone passes. Some of the solvents used Ethanol (200 proof, Pharmco), Methylene Chloride (SpectrAR, Mallinckrodt), and Methylcyclohexane (Omni Solv glass distilled, MCB), were dried over molecular sieve. In addition, cyclohexane was dried over Lithium Aluminum Hydride and distilled under vacuum prior to use. (These precautions were taken to assure that trace amounts of water would not have an effect on the measured kinetics or spectra.) Solutions were prepared to have a ground-state optical density at 355 nm of ≈1.0 in a 1 mm path quartz cell for the ground-state absorption bleaching experiments and of > 2 in 1 mm for the fluorescence experiments. [These ground-state optical densities were chosen to optimize the signal/noise ratio (bleaching experiment) or to minimize detrimental geometrical effects on the time resolution (fluorescence experiments)].

The monodeutero-substituted derivative of (I) was prepared by shaking a solution of (I) in methylcyclohexane with D_2O. Essentially complete exchange of the phenolic hydrogen for deuterium in (I) was confirmed by proton NMR, both before and after the kinetics measurements were made. (This sample was handled in a helium-filled glove bag to prevent contamination by atmospheric H_2O.)

B. Ground-state absorption bleaching recovery kinetics

Absorption recovery kinetics were obtained using a single third-harmonic pulse (Δt = 10 ps, λ = 355 nm) from a modelocked Nd^{3+}: silicate glass laser system. Approximately 90% of the focused UV pulse (excitation pulse) was used to bleach the ground-state absorption of the sample. This pulse, containing ~0.3 mJ, was focused on an ~700 μm diameter aperture at the sample. The remainder of the UV pulse (probe pulse) followed a variable delay line and was used to monitor changes in the sample absorption as a function of time following excitation. The angle between the pump and probe pulse paths was ~6°. The probe pulse absorption by the sample was determined by comparing the intensity of a small portion of the probe pulse, split off prior to passing through the sample, with its intensity after passing through the sample. Pulses were detected on a fast biplanar photodiode with a Tektronix 7904 oscilloscope. Exponential decay curves were fit to the experimental data, after convolution with the excitation and probe pulse widths.

C. Excited-state fluorescence kinetics

The fluorescence kinetics of (I) in several solvents were performed using the streak camera facility of the Regional Laser Laboratory at the University of Pennsylvania. Front surface excitation of the sample was accomplished with the third harmonic of a TEM_{00} modelocked Nd^{3+}: silicate glass laser system. Sample fluorescence, isolated with suitable bandpass filters, was imaged on an ~600 μm pinhole which was in turn imaged on the photocathode of a GEAR Pico V streak camera, used at its maximum streak speed. The streaked fluorescence image was detected and digitized with an ISIT vidicon of an optical multichannel analyzer (PARC, OMA 2). Streak speed and intensity calibration were simultaneously accomplished with a suitably attenuated, second-harmonic pulse which passed through a fixed-separation etalon (l = 6.23 mm). The second-harmonic pulse was diffused and directed to an identical pinhole, whose image was streaked at the same time as the fluorescent image. Using the apparatus in this configuration, an attenuated excitation pulse, scattered from a scattering plate at the sample cell position, had an apparent width of 15 ps. (The actual laser pulse width was ~7 ps, but the streak camera was not used at its maximum time resolution of 2 ps, in order to increase its experimental sensitivity.)

For each sample, at least five separate determinations of fluorescence streaks were obtained. However, only those streaks from clean, single excitation pulses that were suitably "framed" by the streak were considered in the data analysis (i.e., the laser pulse was captured by the camera streak after the first quarter and before the first half of the streak). In some of the experiments (ethanol solvent) the fluorescence intensities were strong enough so that the streaks could be analyzed individually. In other experiments, several streaks were averaged together before data analysis.

For each experiment, the data were analyzed in the following way: (1) The time base calibration was obtained (for individual streaks) by using the simultaneously obtained streaks of etalon-generated peaks to calibrate the channel number in time using an OMA "built-in" cubic function fit. Usually five or six etalon peaks (separated by 41.6 ps) were used in this calibration. (2) For the experiments in which the data were averaged before analysis (methylene chloride and methylcyclohexane solvents), the individual fluorescence streaks that were to be averaged were shifted (in channel number) so that the first etalon peak for each was superimposed at the same channel number. They were then summed in the OMA and an average time calibration determined from the individual etalon tracer. (In general, the variation in etalon peak separation from peak-to-peak and from shot-to-shot was less than ~3%.) (3) The intensity vs time data thus obtained were transferred in digital form from the OMA 2 console to a Hewlett–Packard 85 minicomputer for final data analysis. Also obtained and transferred in a similar way was an experiment of intensity vs time data for a typical, scattered 355 nm laser pulse. (4) Using the H–P 85 computer, experimental fluorescence lifetimes were obtained by deconvolution of the fluorescence kinetics experiments from the detector response to the scattered laser pulse experiment with simultaneous least-squares fitting to an (assumed) exponential decay.[24–27] The data were therefore, least-

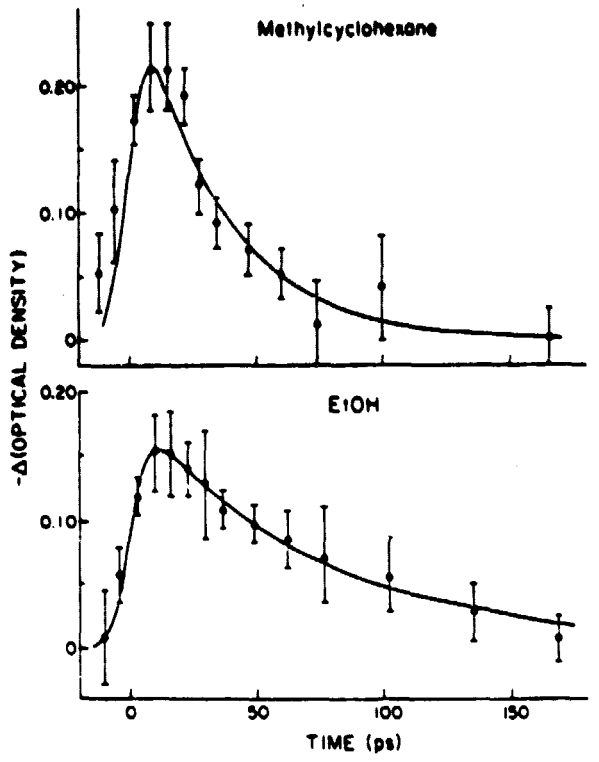

FIG. 2. Transient optical density changes (decreases), due to (I) at 355 nm following excitation at the same wavelength. The sample, in a 1 m cell, had an optical density at 355 nm under low light level conditions of ~1.0. The ⊕ are the average of the experimental optical density changes. The smooth curves are exponential decaying functions, best fit to the data, after convolution to account for the finite duration of the laser excitation and probe pulses. (a) Methylcyclohexane solvent, (b) ethanol solvent.

squares fit with the following function:

$$C(t) = Ae^{-t/\tau}\int_0^t S(t')e^{t'/\tau}dt' + B, \qquad (1)$$

in which

$C(t)$ are the fluorescence intensities as a function of time,

$S(t)$ are the scattered pulse intensities as a function of time,

and A, B, and τ (the lifetime) are adjustable parameters.

(5) Since there was some uncertainty in the position of $t = 0$ (the time position corresponding to the peak of the excitation pulse) in the fluorescence kinetics experiments, the relative time between the fluorescence kinetics experiments and the scattered laser pulse experiment were varied over a range of ~5 ps during the fitting process. The minimum root-mean-square (rms) value determined for each experiment in this range was taken to be the best fit to the data, and the lifetime (τ) determined in this best fit is reported below in Sec. III.

D. Fluorescence spectra and quantum yields

Room temperature emission spectra and quantum yields of (I) in ethanol, methylene chloride, methylcyclohexane, and cyclohexane were obtained under steady-state illumination conditions. Both a Perkin-Elmer MPF3A spectrofluorimeter, fitted with an automatic spectral correction accessory, and another high sensitivity spectrofluorimeter[20] were used in the determinations of fluorescence spectra and quantum yields. In addition, the room temperature emission spectra of (I) in methylcyclohexane and in ethanol were obtained using a conventional laser Raman spectrometer equipped with an argon ion laser Raman spectrometer equipped 363 nm), $f/1.0$ UV collection optics, a 0.85 m double monochromator (Spex 14018), and a cooled photomultiplier (Hamamatsu R955) used in the photon counting mode.

III. EXPERIMENTAL RESULTS

Representative absorption recovery kinetics data at 355 nm for (I) in methylcyclohexane and in ethanol are shown in Figs. 2(a) and 2(b), respectively. Absorption recovery kinetics of (I)d_1 in methylcyclohexane are shown in Fig. 3. The experimental recovery lifetimes, determined in the least-squares fit, are given in the summary in Table I. In all cases, the absorption recovery was complete at the longer delay times investigated with the change in optical density at 355 nm returning to zero within experimental error. No evidence for nonexponential decay behavior was observed in these experiments, again within experimental error.

The fluorescence decay kinetics of (I) in ethanol (fluorescence excited by a single laser shot), methylcyclohexane (fluorescence average due to four laser shots), and methylene chloride (fluorescence average due to three laser shots) are shown in Figs. 4(A), 4(B), and 4(C), respectively. In Fig. 5, the fluorescence intensity vs time data for (I) in ethanol, averaged for five laser shots, are plotted on a semilogarithmic scale, together with the best fit in a least-squares sense of an exponential decay to this data. (Only fluorescence intensity data starting ~25 ps after the peak of the fluorescence intensity are reproduced in this figure.)

The streak-camera-detected fluorescence of (I) in methylcyclohexane and in methylene chloride solvents was somewhat weaker than it was in ethanol solvent.

TABLE I. Summary of room temperature excited-state kinetics in 2-(2′-hydroxy-5′-methylphenyl)-benzotriazole.

Solvent	Absorption recovery τ (ps) at 355 nm	Fluorescence decay τ (ps)
Methylcyclohexane:		
(I)	33 ± 5	14.4 ± 3.4
(I)-d_1	22 ± 5	...
Ethanol	74 ± 10	52.0 ± 3.8
Methylene chloride	29 ± 5	19.1 ± 4.8
Hexadecane	33 ± 3	...

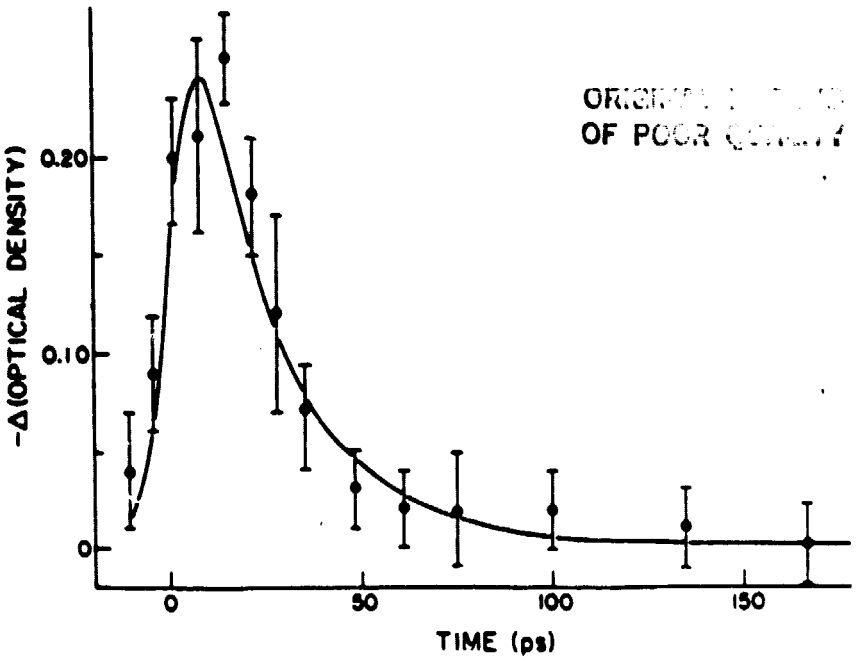

FIG. 3. Transient optical density changes (decreases) of (I)-d_1 in methylcyclohexane at 355 nm. Other conditions were the same as those indicated in the caption of Fig. 1.

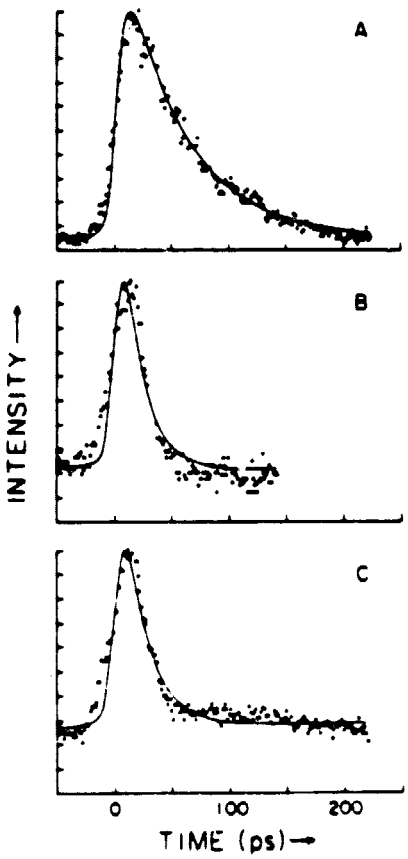

FIG. 4. Streak camera record of the fluorescence intensity ($\lambda \gtrsim 400$ nm) vs time of (I) after excitation at 355 nm; (a) ethanol solvent (single laser shot record), (b) methylcyclohexane solvent (average of four laser shot records), (c) methylene chloride solvent (average of three laser shot records).

This is principally a result of the reduced lifetimes observed in the former solvents.

The values of the fluorescence lifetimes and estimated errors in these lifetimes are given in Table I. These values were obtained as follows: For (I) in ethanol, the value of the lifetime was obtained, as described in Sec. IIC from a least-squares fit to the individual fluorescence decay data for five different laser shots. [One of these five decay data sets is shown in Fig. 4(A).] These values ranged from 48.7 to 58.4 ps. The average value (52.0 ps) and the standard deviation in this average (3.8 ps) are the numbers reported in Table I. For (I) in methylcyclohexane and in methylene chloride, only a single set of averaged decay data were subjected to the least-squares fitting process. [These

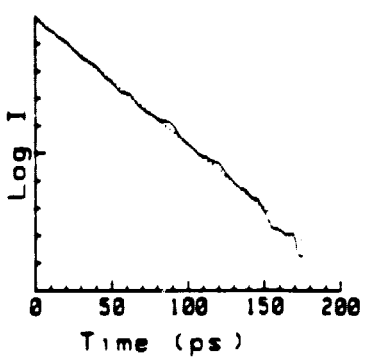

FIG. 5. Semilogarithmic presentation of the fluorescence decay of (I) in ethanol after averaging five laser shot records of the type shown in Fig. 4(a). The dotted curve is a least-squares fit exponential decay ($\tau = 53$ ps) to the experimental data (solid curve). The ordinate scale ranges from 0 to 4.

data sets are shown in Figs. 4(B) and 4(C), respectively.] The lifetime values obtained in these two fits are reported in Table I. The error estimates for these values were obtained by assuming the uncertainty in the position of $t=0$ was ±4 channels (see Sec. IIC) of the OMA (~±2.5 ps), thereby obtaining the range of lifetimes reflected by the error estimates given in Table I. These error estimates were always larger (by ~5×) than the standard deviation in the lifetime parameter obtained in the minimum *rms* (best) fit. (This same procedure was also applied to each single-laser-shot-produced, ethanol solvent data set, and resulted in error estimates, which were approximately the same as the standard deviation in the average reported in Table I. It should be noted that the "best" fits obtained for each single-laser-shot data set established the position of $t=0$ relative to the etalon marker pulse to within ±2 channels from data set to data set.)

In Fig. 4 and for the fluorescent lifetimes given in Table I, the only wavelength discrimination of the fluorescence was provided by a UV blocking filter (Schott, GG 400) to isolate the fluorescence from the laser pulse. For (I) in ethanol only, the short-lived emission was strong enough to allow the use of narrower bandwidth filters to determine the wavelength range of the fluorescence. For example, allowing only emission wavelengths in the range $400\text{ nm} \lesssim \lambda \lesssim 460\text{ nm}$ (Schott GG 400×3 mm, Schott BG 14×3 mm, and Ditric 4600 short-pass cut-off filters), essentially identical emission kinetics were observed for (I) in ethanol as those given in Fig. 4 and Table I. (The best-fit lifetimes for averaged data from three laser shots was in this case 50.1 ps with an error estimate of ±7.8 ps.) On the other hand, for the same sample, blocking all emission wavelengths shorter than ~570 nm (Schott OG 570×3 mm) resulted in a streaked fluorescence signal only barely discernible above background; i.e., less than a few percent of the total short-lived detected visible fluorescence was in a wavelength region to the red of 570 nm. Steady-state emission spectra indicate that fluorescence maxima of (I) in all solvents at room temperature occurs at $\lambda_{max} \lesssim 410$ nm. (See below.)

The short-lived fluorescence kinetics of (I) in ethanol were found to follow an exponential decay, within experimental error, as shown in Fig. 5. The short-lived fluorescence kinetics in methylcyclohexane and methylene chloride were too weak to allow for exact determination of the form of the decay, but were assumed to also be exponential in the fitting procedure.

Broad, featureless emission spectra were observed for (I) in methylene chloride, ethanol, methylcyclohexane, and cyclohexane solvents at room temperature. Initial experiments with the commercial spectrofluorimeter on (I) in the methylene chloride and ethanol solvents indicated very weak emission with maxima in the blue and fluorescence quantum yields on the order of $\sim 2\times10^{-5}$. Subsequently, quantum yield estimates were made using the high sensitivity spectrofluorimeter[28] on (I) in cyclohexane. In this case the emission maximum was at $\lambda_{max} \sim 410$ nm, and the fluorescence quantum yield was estimated to be in the range 2×10^{-6} to 5×10^{-6}. Finally, emission spectra of (I) were obtained with the laser Raman spectrometer (see Sec. IID) in the solvents cyclohexane, methylcyclohexane and ethanol. In every case, the emission maximum occurred in the range $\lambda_{max} \sim 405$–410 nm and the emission intensities were similar. No emission intensity was observed to the red of ~500 nm.

IV. DISCUSSION

A. Excited-state kinetics

The kinetics data presented above provide new information concerning the excited-state decay mechanism of (I). In the first place, in three solvents, the fluorescence decay of (I) was found to occur faster than did the ground-state absorption recovery of (I) at 355 nm. This observation suggests a mechanism involving sequential decay of the fluorescent state through other intermediate state(s) and/or tautomeric form(s) before ground-state recovery is complete. This model might require that the ground-state recovery be somewhat nonexponential but deviations from nonexponential behavior need not be too severe and could easily be masked by the signal-to-noise evidenced by the experimental data (Figs. 2 and 3). From the present ground-state absorption recovery experiments on (I), it is clear that no significant quantum yield of long-lived species is obtained. These results indicate that the major decay pathway involves only singlet species of the molecule.

Another important feature of our results is that both the fluorescence decay and the ground-state absorption recovery lifetimes of (I) are longer in the intermolecular hydrogen bonding solvent (ethanol) than in the non-hydrogen bonding solvents. This observation suggests that the ethanol solvent may competitively form *intermolecular* hydrogen bonds with (I), disrupting the intramolecular hydrogen bond and slowing the excited-state relaxation process as suggested in Sec. I and in Fig. 1.

To investigate the possibility that the kinetics of radiationless deactivation of (I) is affected by solvent viscosity, the ground-state recovery kinetics of (I) was investigated in two different hydrocarbon solvents of different viscosity at room temperature: methylcyclohexane ($\eta = 0.73$ cp) and hexadecane ($\eta = 3.34$ cp). Viscosity-dependent nonradiative rate constants have been determined previously for a number of molecules containing internally rotating phenyl groups.[29–33] If *free* rotation about the C–N single bond joining the phenol and benzotriazole parts of (I) modified its radiationless decay rate in the same way[33] then the decay time observed in hexadecane would be expected to be ~50% longer than in methylcyclohexane. The lack of a viscosity effect on the nonradiative decay rate in (I) suggests that rotation about the C–N bond may be hindered, most likely due to the intramolecular hydrogen bond. In the case of a hindered rotor, it is not clear that the macroscopic viscosity of the solvent is the correct parameter to use in describing the microenvironment of the solute. However, emission studies, discussed below, indicate that the dihedral angle between the phenol

and benzotriazole planes plays a significant role in the decay mechanism.

The effect of deuteration of the hydroxyl group on the rate of relaxation of (I) was investigated using the ground state recovery technique. The measured rate in the deuterated form of (I) was somewhat faster than for the protonated form, although the rates are nearly within experimental error of each other. The fact that a *normal* deuterium isotope effect was not observed indicates that the decay mechanism is not controlled by activated proton transfer or proton tunneling.

B. Emission spectra and quantum yields

A small Stokes shift was obtained for room temperature emission spectra of (I) with $\lambda_{max} \sim 410$ nm in all solvents. The state or species responsible for this emission is not the same one that is responsible for the low temperature, solid phase emission of (I) previously reported in an aprotic matrix[17,18] and confirmed by us ($\lambda_{max} \sim 600$ nm).[34] Whereas, this red emission of (I) in the solid phase is presumably due to a proton-transferred tautomeric form of the molecule, the 410 nm emission in room temperature liquids is probably due to a nonproton-transferred form of the molecule.

The low emission quantum yields observed for (I) in room temperature liquids, however, are not consistent with a purely vertical excited state, one in which the molecular conformation is the same as the ground state's. For example, the radiative lifetime of the vertically excited state of (I) can be obtained, in the conventional picture,[35] by integrating the low energy band(s) of the absorption spectrum. The radiative lifetime, thus determined, turns out to be ~10 or ~4 ns, depending upon whether only the lowest or the two lowest energy bands are included in the integration. This then predicts, for fluorescent lifetimes in the range 14 to 52 ps, that the fluorescence quantum yields should be in the range 10^{-2} to 10^{-3}, or 20 to 500 times larger than actual measured fluorescence quantum yields. Therefore, nonvertical forms of the molecule must be rapidly available from the initially excited form. These forms most likely involve either nonplanar conformations of the molecule or highly excited O–H stretch vibrational states of the molecule as discussed in Sec. IV C below. These forms are probably responsible for the observed room temperature fluorescence of this molecule in liquids.

C. A consistent model for excited-state relaxation

Several groups[4,17–19] have presented a mechanistic model for the singlet decay of (I) which, with slight modification of details, can be shown to be consistent with the known experimental results. The steps in this model are as follows:

$$\begin{aligned} &\text{(a) UV Excitation: } S_0 - S_1, \\ &\text{(b) Proton transfer tautomerization: } S_1 - S_1', \\ &\text{(c) Internal conversion: } S_1' - S_0', \\ &\text{(d) Proton back transfer: } S_0' - S_0. \end{aligned} \tag{2}$$

In this model, S_0 is the ground state of (I); S_1 the initially excited singlet state of (I); S_1' an excited singlet state of a proton-transferred tautomer [e.g., (I′) of Fig. 1]; and S_0' the corresponding ground state of (I′).

Assuming this mechanism is correct, then the room temperature blue fluorescence we report above would be assigned to $S_1 - S_0$ emission, it being only moderately Stokes shifted from the absorption. In fluid solution only this blue fluorescence of (I) is observed. However, when (I) in cyclohexane or methylcyclohexane is cooled somewhat below the melting point of these solvents (~260 and ~200 K, respectively), red emission from (I) has been observed[34] as mentioned in Sec. IV B. This emission, previously observed at 90 K and assigned to $S_1' - S_0'$,[17,18] is not observed in fluid solution. The discrepancy between the measured and calculated fluorescence quantum yields of the blue fluorescence may seem inconsistent with these assignments, however, the model will accommodate these experimental facts as shown below.

While the above data may seem inconsistent, there is in fact a consistent model which neatly rationalizes the experimental observations. The key feature of this model is that the initially excited state of the molecule (S_1) may be in equilibrium with the proton transferred form (S_1') on the picosecond time scale, perhaps by virtue of slow vibrational relaxation in comparison with rapid proton transfer. Therefore, the observed emission is from vibrationally hot molecules of (I) with actual fluorescence quantum yields significantly diminished by dilution with "hot" molecules of the form (I′). (See Fig. 1.) The fluorescence decay time then reflects internal conversion of this (I′) form, which is in equilibrium with the (I) form. Hence, step (2b) above should be written as an equilibrium and step (2c) occurs before vibrational relaxation. The lack of any observable red emission in room temperature fluid solution probably reflects the decreased quantum yield for this process, due to more rapid internal conversion prior to vibrational relaxation. Further, emission of the form $(S_1')^* - (S_0')^*$ might in this model be red-shifted from $S_1' - S_0'$ emission, but it has not yet been observed.

It should be noted that there is evidence in the literature that vibrational relaxation times of large molecules in room temperature solution can be as long as 10–20 ps or so. For example, stilbene in room temperature solution exhibits an excited-state vibrational relaxation time of ~25 ps[36] while in dibenzpyrene, this time has been estimated as ~15 ps.[37] Whether excited-state vibrational relaxation times of (I) in room temperature solution can be slower than ~15 ps is still an open question, but the spectroscopic evidence cited above tends to confirm that they can be. (In ethanol, slowing of the equilibration process by competing intermolecular hydrogen bonding extends the fluorescence decay and the model does not really require that vibrational relaxation in ethanol be as slow as 50 ps, only that the equilibrium process be rate determining.)

Other experimental results are readily accommodated

by this model. The fluorescence decay times are shorter than the ground-state recovery times because most molecules evolve into proton-transferred ground-state forms of (I'), i.e., S_0'. Ground-state recovery times then include the additional time for step (2d) of back proton transfer so that both internal conversion and back transfer contribute to the observed rate. The observation that fluorescence decay times are slowed in ethanol probably reflects the slowing of establishment of equilibrium in step (2b), due to the interferring nature of the intermolecular hydrogen bonds formed by the solvent with (I). Internal conversion rates would also be expected to change, since the solvent modifies the excited-state potential surface.

The viscosity effect is not quite so clear cut. Internal phenol rotation in this molecule is, at best, hindered and the microscopic viscosity dependence of this motion may be weaker than in molecules which undergo free internal rotation. Thus, it might be argued that step (2c) is promoted by relative librational motion of the phenol and benzotriazole portions of the molecule. Evidence concerning the importance of this librational motion on the rate of internal conversion manifests itself in the observation of relaxed red fluorescence in aprotic rigid matrices in which the amplitude of the relative motion would be less than in fluid solution. In any case, the ground-state recovery times measured in hexadecane and methylcyclohexane give the rates of composite processes, and hence may not be very sensitive to the modest viscosity difference in these two solvents.

The deuteration effect on ground-state recovery times eliminates rate-determining proton tunneling or activated proton transfer from the excited-state relaxation model. In the proposed model, it is not clear what the effect of deuteration of the molecule should have on the rate of the overall process of internal conversion and back proton transfer [steps (2c) and (2d)]. For example, the rates of internal conversion processes depend on the density of vibronic states and Franck–Condon factors of the lower energy state to which decay occurs. These factors could conceivably be affected by deuteration in such a way that the radiationless process would be more rapid in the deutero derivative than in the proto, so the model is consistent with the experimental observations.

Other workers have reported kinetic solvent effects on the relaxation of similar molecules. For example, a similar solvent effect was observed on ground state recovery kinetics reported for 2-hydroxybenzophenone.[11] In that molecule, complete ground-state recovery was determined to occur exponentially with a lifetime of 35 ± 5 ps in hexane solvent. In ethanol, however, the ground-state absorption recovery proceeded in a nonexponential fashion: a fast component of ~30 ps and a slow component of 1.5 ns.[11] For that molecule, the authors proposed the presence of two different ground-state species in ethanol (e.g., an intramolecular hydrogen-bonded molecule and a molecule intermolecularly hydrogen-bonded to the solvent) as a possible explanation of the results. The long time component of the ground-state recovery was assigned to a triplet decay route, tentatively attributed to those molecules hydrogenbonded to the solvent. In the present ground-state absorption recovery experiments on (I), however, no long-lived species were observed, either in ethanol or the other solvents. Furthermore, although the possibility of more than one ground-state species cannot be ruled out for (I) in ethanol, there is no evidence in either the fluorescence or the ground-state recovery kinetics for nonexponential decay. Therefore, there is no reason to invoke more than one ground-state form of (I) in ethanol.

Recently, Smith and Kaufmann[9] presented a model which considers the effect of the dielectric strengths of the solvent on the nonradiative decay rate of the related molecule methyl salicylate. In contrast to the present results, they observe *shorter* fluorescence lifetimes in hydrogen-bonding solvents than in hydrocarbons. They attribute this to an increased intersystem crossing rate in these solvents caused by a decreased singlet–triplet energy gap in the zwitterionic form of the molecule. In the case of (I), there is no experimental evidence that intersystem crossing is a significant radiationless decay route in room temperature fluid solution, nor is any highly Stokes shifted (zwitterionic) emission of (I) observed under these conditions.

In conclusion, the kinetic and spectroscopic data presented above provide new information concerning the excited-state decay mechanism of (I). The model of this decay mechanism is as follows:

$$\begin{aligned}
&\text{(a) UV excitation: } S_0 - S_1^*, \\
&\text{(b) Proton transfer tautomerization: } S_1^* \rightleftarrows (S_1')^*, \\
&\text{(c) Internal conversion: } (S_1')^* - (S_0')^*, \text{ and} \\
&\text{(d) Vibrational relaxation and proton back transfer: } (S_0')^* - S_0 ,
\end{aligned} \tag{3}$$

in which "′" indicates a proton-transferred form and "*" a vibrationally unrelaxed state. Fluorescence of (I), observed in room temperature fluid solution with a normal Stokes shift, is attributed to a vibrationally unrelaxed excited state S_1^*, which is in equilibrium with the proton-transferred excited state $(S_1')^*$ of the molecule. Internal conversion $(S_1')^* - (S_0')^*$ controls the lifetime of this fluorescence, while ground-state recovery rates include additional contributions from vibrational relaxation and proton back transfer in the ground state.

ACKNOWLEDGMENTS

We wish to thank Professor Robin Hochstrasser, Director of the Regional Laser Laboratory at the University of Pennsylvania, for providing to us the opportunity to conduct the streak camera measurements of fluorescence decay in that laboratory. We appreciate the expert guidance and assistance of Mr. Dan Negus during the course of these experiments at the Regional Laser Laboratory. One of us (GWS) wishes to thank Professor Bryan Kohler for helpful discussions regarding this work and for his warm hospitality

at Wesleyan University. We also thank Ms. Linda DeLucci for preparation of the manuscript.

[1]J. R. Merrill and R. G. Bennett, J. Chem. Phys. 43, 1410 (1965).
[2]A. A. Lamola and L. J. Sharp, J. Phys. Chem. 70, 2634 (1966).
[3]J. P. Guillory and C. F. Cook, J. Am. Chem. Soc. 95, 4885 (1973).
[4]J. A. Otterstedt, J. Chem. Phys. 58, 5716 (1973).
[5]W. Klöpffer, Adv. Photochem. 10, 311 (1977).
[6]H. Shizuka, K. Matsui, Y. Hirata, and I. Tanaka, J. Phys. Chem. 80, 2070 (1976); 81, 2243 (1977).
[7]K. K. Smith and K. J. Kaufmann, J. Phys. Chem. 82, 2286 (1978); and in *Laser Chemistry*, edited by A. H. Zewail (Springer, Berlin, 1978), p. 163.
[8]D. Ford, P. J. Thistlethwaite, and G. J. Woolfe, Chem. Phys. Lett. 69, 246 (1980).
[9]K. K. Smith and K. J. Kaufmann, J. Phys. Chem. 85, 2845 (1981).
[10]P. J. Thistlethwaite and G. J. Woolfe, Chem. Phys. Lett. 63, 401 (1979).
[11]S.-Y. Hou, W. M. Hetherington III, G. M. Korenowski, and K. B. Eisenthal, Chem. Phys. Lett. 68, 282 (1979).
[12]C. Merritt, G. W. Scott, A. Gupta, and A. Yavrouian, Chem. Phys. Lett. 69, 169 (1980).
[13]A. Gupta, A. Yavrouian, S. DiStefano, C. D. Merritt, and G. W. Scott, Macromolecules 13, 821 (1980).
[14]A. Gupta, G. W. Scott, and D. Kliger, ACS Symposium Series 151 (ACS, Washington, 1980), Chap. 3.
[15]A. L. Huston, C. D. Merritt, G. W. Scott, and A. Gupta, in *Picosecond Phenomena II*, edited by R. M. Hochstrasser, W. Kaiser, and C. V. Shank (Springer, Berlin, 1980), p. 232.
[16]K. J. Choi, L. A. Halliday, and M. R. Topp, in Ref. 15, p. 131.
[17]T. Werner, J. Phys. Chem. 83, 320 (1979).
[18]T. Werner, G. Wössner, and H. E. A. Kramer, ACS Symposium Series 151 (ACS, Washington, 1980), Chap. 1.
[19]T. Werner and H. E. A. Kramer, Europ. Polym. J. 13, 501 (1977).
[20]A. U. Acuña, F. Amat-Guerri, J. Catalán, and F. González-Tablas, J. Phys. Chem. 84, 629 (1980), and references therein.
[21]L. A. Heimbrook, J. E. Kenny, B. E. Kohler, and G. W. Scott, J. Chem. Phys. 75, 5201 (1981).
[22]H. J. Heller, Europ. Polym. J. Suppl. 105, 105 (1969).
[23]B. Ranby and J. F. Rabek, *Photodegradation, Photooxidation, and Photostabilization of Polymers: Principles and Applications* (Wiley, New York, 1975).
[24]S. S. Brody, Rev. Sci. Instrum. 28, 1021 (1957).
[25]A. Hang, B. E. Kohler, E. B. Priestly, and G. W. Robinson, Rev. Sci. Instrum. 40, 1439 (1969).
[26]J. N. Demas and G. A. Crosby, Anal. Chem. 42, 1010 (1970).
[27]W. R. Ware, in *Creation and Detection of the Excited State* 1A, edited by A. A. Lamola (Marcel Dekker, New York, 1971), Chap. 5.
[28]S. F. Rice and H. B. Gray (unpublished results).
[29]C. V. Shank, E. P. Ippen, O. Teshke, and K. B. Eisenthal, J. Chem. Phys. 67, 5547 (1978).
[30]Th. Förster and G. Hoffman, Z. Phys. Chem. (Leipzig) 75, 63 (1971).
[31]D. Magde and M. W. Windsor, Chem. Phys. Lett. 24, 144 (1974).
[32]E. P. Ippen, C. V. Shank, and A. Bergman, Chem. Phys. Lett. 38, 611 (1976).
[33]W. Sibbett, J. R. Taylor, and D. Welford, IEEE J. Quantum Electron. 17, 500 (1981).
[34]A. L. Huston and G. W. Scott (unpublished results).
[35]S. J. Strickler and R. A. Berg, J. Chem. Phys. 37, 814 (1962).
[36]B. I. Greene, R. M. Hochstrasser, and R. B. Weisman, Chem. Phys. Lett. 62, 427 (1979).
[37]K.-J. Choi and M. R. Topp, Chem. Phys. Lett. 69, 441 (1980).

Appendix (II)

Picosecond kinetics of excited state decay processes in internally hydrogen-bonded polymer photostabilizers

Alan L. Huston, Gary W. Scott
Department of Chemistry, University of California/Riverside, Riverside, California 92521

Abstract

We report results of recent measurements of excited state decay kinetics in molecules which are commonly used as commercial polymer photostabilizers. Discussion centers on molecules in the 2-(2'-hydroxyphenyl)-benzotriazole and 2-hydroxybenzophenone classes. Determination of room temperature fluorescence decay, transient absorption and ground state absorption recovery kinetics are presented. In addition, low temperature spectra and variable temperature fluorescence decay kinetics are also presented. Solvent effects on the spectra and kinetics give considerable insight into the radiationless processes that occur in these systems.

Introduction

Most polymers are photochemically affected by solar ultraviolet radiation, especially after long term exposure. Economically practical solar energy conversion devices should be constructed from inexpensive, visible-radiation transparent, durable, light-fast materials. Plastics that are not particularly susceptible to solar ultraviolet degradation (e.g. fluorocarbons, methylsilicones, and certain acrylics) are, in general, expensive to manufacture and do not possess optimum mechanical and/or optical properties for these applications. Less expensive, more durable, and optically transparent plastic films which would otherwise be ideal for mechanically protecting, e.g., a photovoltaic array are, in general, quite susceptible to photochemical deterioration upon exposure to solar radiation. These polymers tend to crack, become cloudy, and turn yellow as photochemical degradation occurs, causing a significant decrease in the amount of useful, visible solar radiation that can reach the solar collector for conversion to electrical energy. Thus, the useful lifetime of the device is shortened by the plastic coating that protects it.

Fortunately, there are well-known techniques available for protecting polymers from photochemical degradation.[1,2] These techniques involve the modification of the composition or structure of polymeric material by incorporation of photostabilizers. Such molecules provide photostabilization by selectively absorbing solar ultraviolet radiation, thus preventing excitation of the photochemically reactive chromophores of the polymer. In addition, photostabilizers are transparent in the visible portion of the solar spectrum, allowing most of this nonphotochemically-damaging radiation to pass through the polymer. Ideal photostabilizers also serve as energy acceptors to quench excited-state polymer chromophores before photochemical damage can occur. Furthermore, photostabilizer excited states, must rapidly relax in a manner that converts the excitation energy into a form (in most cases heat) that is not chemically damaging to the polymer. Finally, the photostabilizers themselves must be nonphotochemically reactive.

A common method of protecting polymers is to use a photostabilized polymeric film as a coating on the bulk polymer. For example, transparent acrylic films may be made by incorporating photostabilizers into polymethylmethacrylate. The photostabilizing effectiveness of monomeric forms of photostabilizers may be less than expected for two practical reasons: (1) The monomeric photostabilizers blended into the polymer may be lost by evaporation and/or leaching. (2) Aggregation is a common problem when monomers are incorporated into polymers, providing nonuniform protection.

There are two classes of widely-used, ultraviolet-absorbers that are used as commercial photostabilizers and which have in common the molecular structural feature of an intramolecular hydrogen bond. These two classes of molecules--2-hydroxybenzophenone (HB) and 2-(2'-hydroxyphenyl)benzotriazole (HPB)--are shown in Figure 1.

The intramolecular hydrogen bond in these photostabilizing molecules is believed to be instrumental in the rapid conversion of the absorbed ultraviolet radiation into nonphotochemically damaging heat. The present study is concerned with the kinetics and mechanism of such processes in several of these molecules whose structures are given in Figure 1. Three monomers (HB-I, HPB-I and HPB-II) were studied. Also, for comparison, we investigated two polymeric photostabilizers. These were obtained by copolymerizing an appropriate allyl or vinyl derivative of one of the parent compounds, HB-II[3] or HPB-III[4], with methyl methacrylate. These copolymers will be referred to below as coHB-II:MMA and coHPB-III:MMA, re-

spectively.

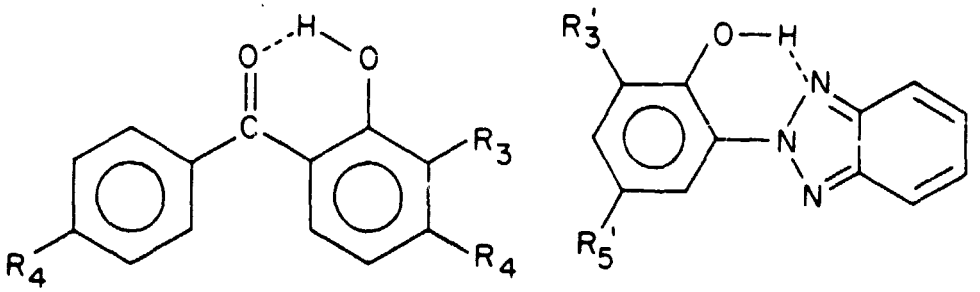

HB HPB

Figure 1. Molecules investigated.
HB-I. 2-hydroxybenzophenone ($-R_3$ & $-R_4$:-H)
HB-II. 2-hydroxy,3-allyl,4,4'-dimethoxybenzophenone ($-R_3$:$-CH_2-CH=CH_2$; $-R_4$:$-OCH_3$)
HPB-I. 2-(2'-hydroxy-5'-methylphenyl)-benzotriazole ($-R'_3$:H; R'_5:$-CH_3$)
HPB-II. 2-(2'-hydroxy-3',5'-di-tert-amylphenyl)benzotriazole (R'_3 & R'_5:$-C(CH_3)_2-CH_2-CH_3$)
HPB-III. 2-(2'-hydroxy-5'-vinylphenyl)benzotriazole ($-R_3'$:-H; $-R_5'$:$-CH=CH_2$)

Within each class of compounds, the differences in molecular structure should not really be important in determining their inherrent photostabilizing effectiveness. However, as alluded to above, the molecular structure may affect their solubility, limiting the concentration and uniformity of distribution of these molecules in the polymer, thus limiting the real photostabilizing effectiveness.[5,6] The polymeric forms of these photostabilizers--coHB-II:MMA and coHPB-III:MMA--have therefore certain advantages in this respect over the monomeric photostabilizing molecules.[3,4,6]

In the present study we report the results of several types of spectroscopic and kinetics measurements which relate directly to the mechanism of excited-state relaxation of polymer photostabilizers in the class HB and HPB (See Fig. 1). Several of these results have been previously reported.[3,4,6-9] In combination with the new results presented below for the first time, a clear mechanistic model for excited state decay of these photostabilizers and the kinetics of the processes is obtained. This model involves excited state intramolecular proton transfer or tautomerization, possibly to a zwitterionic form. Results from others were also used in the development of this model.[10-17]

Absorption Spectra and Recovery Kinetics

Ground State Molecules

Spectra. For molecules in classes HB and HPB there is a relatively strong uv absorption which exhibits maximum extinction coefficients in the range 5,000 - 20,000 $l\ mol^{-1}cm^{-1}$. These absorption bands, peaking at wavelengths of ~340-350 nm, occur in molecules in the HB and HPB classes, but not in related molecules which do not have substituents like o-hydroxyphenyl groups available for intramolecular hydrogen bonding. Hence, excitation into these absorption bands occurs, predominantly, for molecules which may be in ground state intramolecularly hydrogen-bonded conformations. These conclusions are supported by our observations on molecule HPB-I which indicate that the extinction coefficient decreases by 30-40% upon going from methylcyclohexane solvent to the strong intermolecular hydrogen bonding solvent, trifluoroethanol. The reduction in extinction coefficient is considerably less in ethanol, but the wavelength at the peak is blue-shifted by 10 nm (ethanol) and 15 nm (trifluoroethanol) relative to methylcyclohexane solvent.

Kinetics. Ground state absorption recovery kinetics were investigated for class HPB type molecules using a single third harmonic pulse (~10 ps) from a modelocked, Nd^{+3}:glass laser system to both excite and probe the absorption recovery at 355 nm. Similar measurements have been reported on HB-I by another group.[17] The results of our measurements on the HPB class molecules are reported in Table 1 below.

For all of the ground state absorption recovery kinetics determined on room temperature solutions of HPB type molecules (Table 1), the recovery kinetics were always essentially exponential in form and complete at the longest delay times investigated in all solvents. An example of this behavior is shown in Figure 2 for HPB-I in methylene chloride.

Table 1. Ground State Absorption Recovery Times of HPB Class Molecules in Room Temperature Solution

Molecule (See Fig. 1)	Solvent	Recovery Time (ps)
HPB-I	Methylcyclohexane	33±5
	Ethanol	74±10
	Methylene Chloride	29±5
	Hexadecane	33±5
HPB-II	Methylcyclohexane	40±15
coHPB-III:MMA	Methylene Chloride	25±5

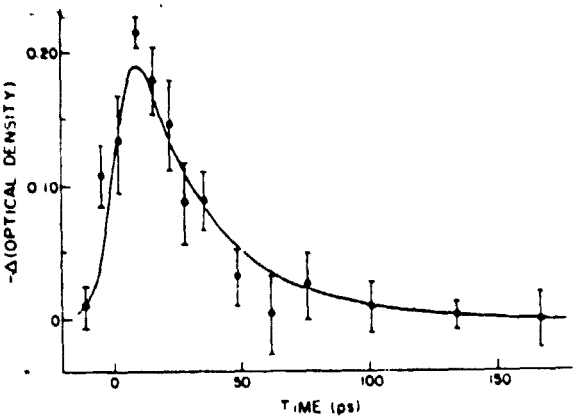

Figure 2. Ground state absorption recovery kinetics of HPB-I at 355 nm in methylene chloride solution.

For type HB photostabilizers, Fisenthal and his group[15] have investigated the ground state absorption recovery kinetics of HB-I in protic and aprotic solvents (ethanol and hexane, respectively). In that molecule, complete ground state recovery was observed in hexane solvent with single exponential kinetics (τ=35±5 ps), whereas in ethanol, ground state recovery kinetics of HB-I occurred in two steps: a fast component of ~30 ps and a slower, ~1.5 ns recovery step. In the ethanol solvent the authors proposed that HB-I molecules could have two ground state conformations: intramolecularly hydrogen-bonded and intermolecularly hydrogen-bonded, the former conformation giving rapid ground state recovery and the latter yielding slower recovery through, e.g., a triplet decay route. This picture has been disputed recently, however, by Topp and his group[16] who contend that only one type of HB-I (intermolecularly hydrogen-bonded) exists in ethanol. (See next section.)

Transient Species

We have previously reported transient absorption spectra of both the HB[7,8-9] and HPB[7,8] classes of photostabilizers in room temperature solution. These spectra are quite difficult to obtain with high signal-to-noise ratios due to the low absorbances obtained in the visible region of the spectrum. These spectra have been obtained by excitation with a single third-harmonic pulse from a modelocked, Nd^{+3}:glass laser system. Time-delayed continuum probe pulses were generated by focussing the fundamental pulse into a suitable liquid. Single-shot transient spectra were obtained, double-beam-corrected, with a polychromator optical multichannel analyzer (OMA 2, EG&G PARC) combination.

A summary of these results is as follows: For HB type molecules in essentially aprotic solvents (methylene chloride and isooctane) weak transient absorption in the 400-700 nm range were observed at short delay times (t ≤ 50 ps) following excitation with absorption maxima in the blue region of the spectrum (λ_{max} ~420-450 nm). These observations obtained for solutions of both HB-I and coHB-II:MMA. For HB class molecules in a protic solvent (ethanol), a longer-lived transient absorption in the same wavelength region was observed for delay times in excess of 400 ps. Related kinetics studies by Topp's group[16] indicate that there are distinct differences in the decay of the initially excited singlet state of HB-I in different solvents. For HB-I in hexane they report ~6 ps whereas in ethanol they report ~30 ps, based on transient absorption detected with their upper-state fluorescence technique.

For HPB type photostabilizers, broad weak transient visible absorption was observed at short delays (t ≤ 20 ps; λ_{max} ~440 nm) in both methylene chloride and ethanol. Longer-lived transient absorption, which we previously reported,[7] has not been confirmed by subsequent experiments. These measurements have, at present, only been made on the monomeric photostabilizers in this class (HPB-I and HPB-II). However, additional measurements of this type made on 2-(2'-acetoxy-5'-methylphenyl)benzotriazole[9] confirm that the short time transient absorption observed in HPB-I is probably due to a conformation of the molecule in which proton transfer is not yet complete.

Emission Spectra and Kinetics

Emission Spectra

We have obtained emission spectra of HPB type photostabilizers both in room temperature fluid solution and also in low temperature matrices. Low temperature emission spectra in

these molecules have also been previously reported by Otterstedt[13] and by Werner.[16] Very little is known about the apparently quite low quantum yield fluorescence of HB class molecules, although some highly Stokes-shifted low temperature emission of derivatives of HB have been reported. Low temperature phosphorescence of HB-I was reported a number of years ago by Lamola and Sharp.[10]

Room Temperature Fluorescence. Room temperature spectra of HPB-I in fluid solution have been obtained in both protic (ethanol) and aprotic (methylene chloride, methylcyclohexane and cyclohexane) solvents. Typically, excitation was accomplished with uv lines from an argon ion laser with a high sensitivity spectrofluorimeter used to obtain the emission spectra. Broad, featureless emission spectra were observed for HPB-I in the blue region of the visible. Typically, the emission peak occurred at λ_{max} ~405-410 nm in both protic (ethanol) and aprotic (methylcyclohexane) solvents. The emission intensity tailed off to the red with little or no emission observed beyond ~500 nm. Quantum yields of emission were estimated to be in the range $2\text{-}5\times10^{-5}$.

Low Temperature Emission. At low temperatures, emission spectra of both HB[10,11] and HPB[11,14] type photostabilizers are qualitatively similar. In protic (alcoholic) glasses, "blue" fluorescence with only a moderate Stokes shift and long-lived "blue/green" phosphorescence have been observed. On the other hand, in aprotic (hydrocarbon) solvents, only highly Stokes-shifted, "red" fluorescence and no phosphorescence has been observed. (In some cases, e.g., HB-I, no fluorescence is observed at all in low temperature hydrocarbon matrices, and only phosphorescence and no fluorescence is observed for the HB class molecules in alcoholic glasses.)

We have investigated, primarily, the emission spectra of 2-(2'-hydroxy-5'-methylphenyl)-benzotriazole in low temperature solid matrices. In this case, the observed emission was much stronger than in fluid solutions at room temperature. These measurements were obtained by cooling the sample solution down in a round quartz cell which was in good thermal contact via a coaxial brass rod with the cold stage of a variable temperature, closed cycle helium refrigerator (Air Products, Displex 202E). Sample excitation was accomplished with the 325 nm line of a HeCd laser (Liconix 4050/4055) with emission spectra obtained with a scanning 1 m monochromator (Hilger-Engis 1000) and a red-sensitive photomultiplier used in the current detection mode. Typical spectra obtained for HPB-I are shown in Figure 3. In the highly cracked, ethanol glass, the portions of the spectrum marked F and P correspond to the fluorescence and phosphorescence of HPB-I, respectively.

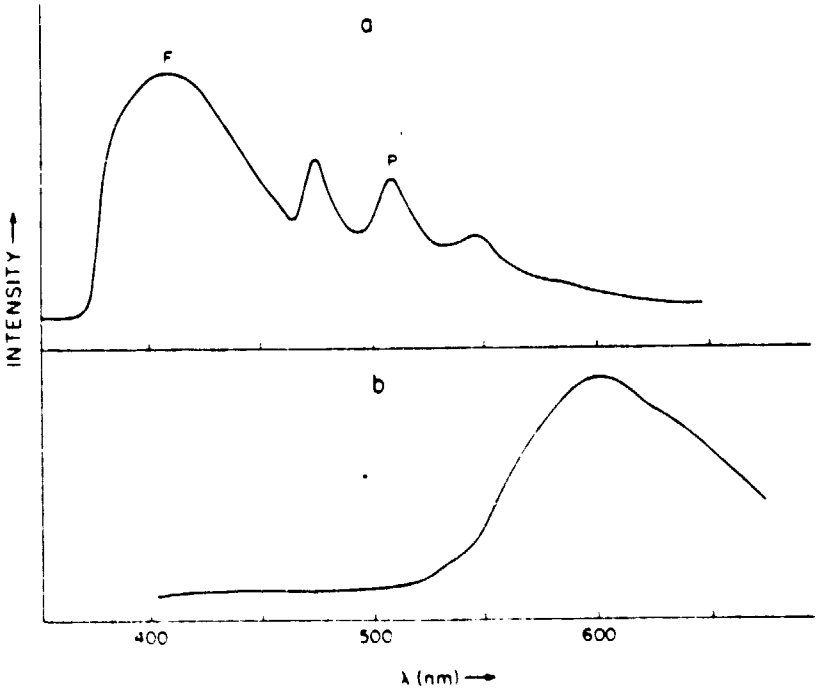

Figure 3. Emission spectra of 2-(2'-hydroxy-5'-methylphenyl)-benzotriazole (HPB-I) in (a) ethanol and (b) methylcyclohexane, both at 12K. In (a), the P (phosphorescence) portion of the spectrum exhibits an ~0.5 sec lifetime while the F (fluorescence) portion decays on the nsec time scale. These spectra are not corrected for instrument response.

These spectra are similar to those previously reported by Werner[16,17] for HPB-I in protic and aprotic glasses at 90K. We have, however, also investigated the temperature dependence of the "red" emission of HPB-I in a cracked, n-octane glass over the temperature range 11-169K. The fluorescence maximum occurred at ~625 nm, and did not shift with temperature. However, the fluorescence intensity was strongest at the lowest temperature and decreased significantly upon warming, being only observable below the temperature of rigid glass formation.

Fluorescence Kinetics

Room Temperature Solutions. The kinetics of the room temperature fluorescence of HPB-I and coHPB-III:MMA in solution were measured, following excitation by a third harmonic pulse from a modelocked Nd^{+3}:glass laser system, with a streak camera. The details of these measurements, data analysis and results for HPB-I are being presented elsewhere.[9] Briefly, the streak camera was operated with a time resolution of ~15 ps; however, by deconvolution techniques lifetimes down to this time range could be determined.

For the copolymer of the HPB class molecules (coHPB-III:MMA), fluorescence decay measurements were obtained in room temperature methylene chloride solution. Although the decay was too rapid to obtain its exact form, deconvolution from the excitation pulse profile as observed by the detection system, gives a reasonably accurate estimate of the fluorescence lifetime, assuming single exponential decay. The fluorescence decay data obtained (dots) together with a convoluted, least-squares best fit to this data (solid line) are shown in Figure 4 for coHPB-III:MMA in methylene chloride. Fluorescence lifetimes obtained from this fit and analogously for HPB-I in several solvents are given in Table 2.

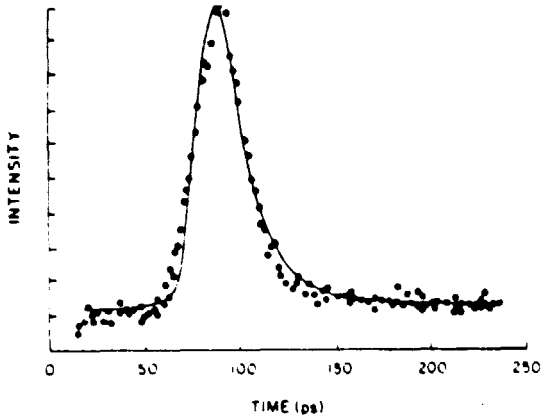

Figure 4. Fluorescence decay kinetics of coHPB-III:MMA in methylene chloride at room temperature.

Table 2. Fluorescence Lifetimes of HPB Class Molecules in Room Temperature Solution

Molecule (See Fig. 1)	Solvent	Fluorescence Lifetime (ps)
HPB-I	Methylcyclohexane	14±3
	Ethanol	52±4
	Methylene Chloride	19±5
coHPB-III:MMA	Methylene Chloride	15±4

It should be noted that in every case investigated, the fluorescence lifetimes are shorter than the ground state recovery times for the same molecule in room temperature solution. (Compare Tables 1 and 2.) Also, the polymeric form of the HPB class has a similar lifetime as the monomeric forms in aprotic solvents. However, the fluorescence and ground state recovery times are significantly longer in ethanol than in the aprotic solvents. Fluorescence decay kinetics in HB class photostabilizers have not been investigated.

Temperature Dependence of the Red Emission. The kinetics of the fluorescence decay of the "red" fluorescence of HPB-I in low temperature hydrocarbon matrix (n-nonane) are reported here for the first time. These kinetics were measured after excitation, again with a 355-nm, 10-ps laser pulse, by observation of the red fluorescence through suitable filters with a fast, biplanar photodiode while photographically recording the diode output from a Tektronix 7904 oscilloscope. Temperature variation of the sample was accomplished with the closed cycle refrigerator described above. Lifetimes were obtained, after digitization of the photographic decay data, with L.S.F. deconvolution by computer in much the same manner as was the streak camera data as described above and in our recent work.[9] Lifetimes were obtained for both the molecule HPB-I and its monodeuterated analog (HPB-I-d_1), obtained by shaking a solution of HPB-I in n-nonane with excess D_2O. This HPB-I-d_1 molecule has a deuterium replacing the hydrogen in the hydroxy group of the phenolic ring of HPB-I (See Fig. 1).

A typical set of "red" fluorescence decay data (dots) for HPB-I in n-nonane, obtained at 100K, is shown in Figure 5 below. The L.S.F. convolution (solid line) yields an (assumed) exponential decay lifetime of 630 ± 60 ps.

Below approximately 30K, the fluorescence lifetimes determined were temperature independent. Above this temperature, the lifetimes decreased with increasing temperature. Further, at all temperatures for which the lifetime could be reliably determined, the lifetime of HPB-I was always less than or equal to the lifetime of HPB-I-d_1. These results suggest that the following model of excited state decay should be applicable in this system:

$$k_{tot} = k_r + k_{nr}, \tag{1}$$

in which k_{tot} is the rate constant governing decay of the red-emitting state, k_r is the radiative decay rate constant and k_{nr} is the nonradiative decay rate constant. The nonradiative decay rate should have both a temperature-dependent and temperature-independent part since the radiative rate is not expected to depend on deuteration. Therefore, the nonradiative rate constant is given by the following:

$$k_{nr} = k_{nr}' + k_{nr}'(T), \tag{2}$$

in which the second term on the right-hand-side includes all of the temperature dependence of the nonradiative relaxation processes. Assuming all of the nonradiative relaxation temperature dependence is associated with a single activation energy, then $k_{nr}'(T)$ can be written as

$$k_{nr}'(T) = A_{nr}e^{-\Delta E_{nr}/kT}, \tag{3}$$

in which ΔE_{nr} is the activation energy required for this process.

The temperature independent contributions tc k_{tot} for both HPB-I and HPB-I-d_1 were obtained by subtracting the measured k_{tot} at 12K from the measured k_{tot} at all other temperatures. The values of the measured lifetimes obtained and a plot of ln $k_{nr}'(T)$ vs 1/T are given in Table 3 and Figure 6.

The fluorescence decay kinetics of HPB-I in the solid matrix are apparently strongly influenced by a nonradiative process. It seems quite reasonable to attribute this fluorescence to a tautomeric, proton-transferred form of HPB-I (See below). Also the nonradiative decay process which is rate-controlling is likely internal conversion of the excited

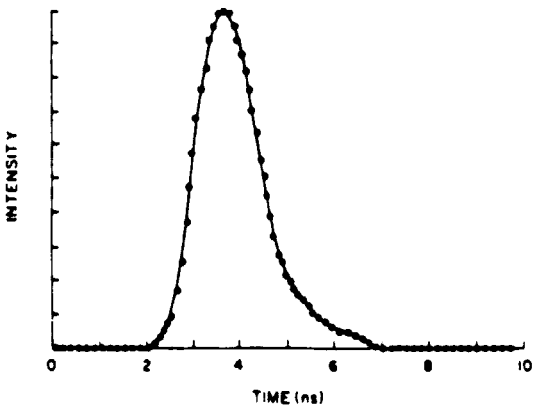

Figure 5. Fluorescence decay kinetics of HPB-I in n-nonane at 100K.

Table 3. Fluorescence Lifetimes of 2-(2'-hydroxy-3'-methylphenyl)benzotriazole (HPB-I) in n-nonane as a function of temperature

T (K)	τ of HPB-I (ns)	τ of HPB-I-d_1 (ns)
12	.82±.07	1.2±.1
90	.71±.07	.85±.1
100	.63±.06	.87±.08
110	.56±.06	.85±.08
120	.58±.06	.66±.06
130	.52±.06	.61±.06
140	.41±.06	.60±.06
150	--	.64±.06
159	--	.59±.06
179	--	.39±.06

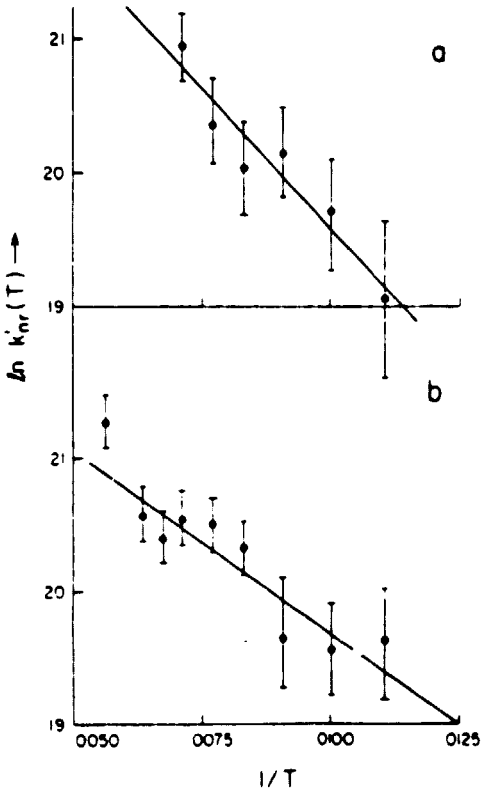

Figure 6. Plot of ln $k'_{nr}(T)$ vs. 1/T for (a) HPB-I and (b) HPB-I-d_1 in n-nonane. (See text for details.)

singlet (to ground singlet) of this tautomer. Activation energies (equation (3)) obtained by linear least squares fit to the data displayed in Fig. 6 are $\Delta E_{nr}(HPB\text{-}I)/hc = 282 \pm 43$ cm^{-1} and $\Delta E_{nr}(HPB\text{-}I\text{-}d_1)/hc = 193 \pm 33$ cm^{-1}. The differences in these activation energies suggest involvement of a vibrational normal mode which includes N-H (N-D) or O-H (O-D) motion. However, these differences are only slightly outside of the combined experimental errors.

Mechanistic Interpretation

Considering the experimental data presented above, we propose a model for excited state deactivation of HPB-I which is a slightly modified version of the model proposed earlier by Otterstedt[13] and Werner.[16] The overall mechanism that they proposed may be written as follows:

$$S_0 \xrightarrow{h\nu} S_1 \xrightarrow[\text{transfer}]{H^+} S_1' \xrightarrow{ic} S_0' \xrightarrow[\text{transfer}]{H^+} S_0. \qquad (4)$$

The major steps in the mechanism following absorption of the uv light are first of all proton transfer to give the zwitterionic form, S_1', followed by rapid internal conversion to give the proton transferred ground state form S_0' which then rapidly equilibrates to give the ground state form, S_0. The new kinetic and spectroscopic evidence that we presented above allows us to provide a more detailed account of the mechanism. The basic processes involved are shown schematically in Figure 7.

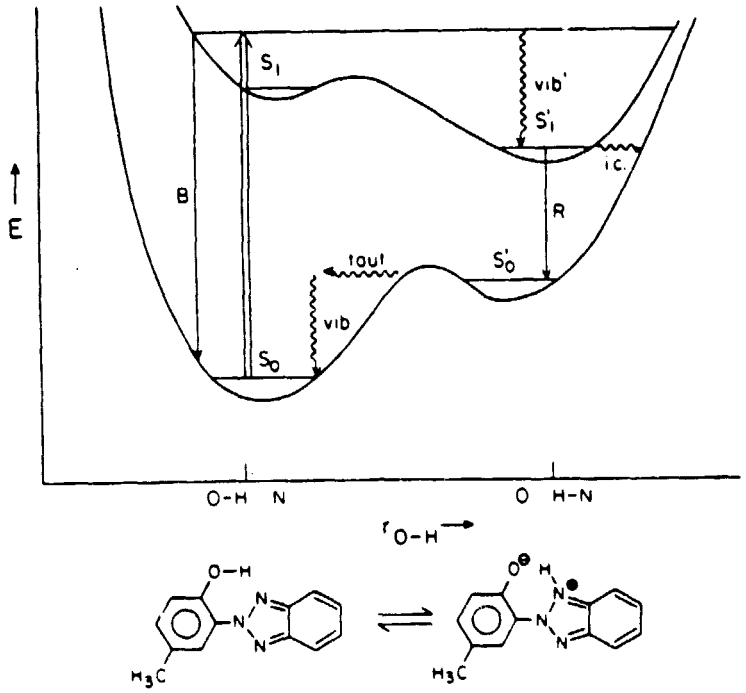

Figure 7. Potential energy surfaces and details of the absorption and excited state deactivation processes in HPB-I.

Based on the absorption spectrum of HPB-I in aprotic solvents, compared to its spectrum in the strongly hydrogen-bond-breaking trifluoroethanol solvent, we assert that the absorption band at 350 nm is primarily due to the intramolecularly hydrogen-bonded form of HPB-I. Absorption at 355 nm produces an excited vibrational level in S_1. Room temperature fluorescence spectra and kinetics in hydrocarbon solution exhibit blue emission (B), λ_{max} ~410 nm, τ ~ 14 ps with an estimated quantum yield of $2\text{-}5 \times 10^{-5}$. Ground state recovery kinetics measure the rate of the overall process to be ~30 ps in hydrocarbons. We propose that the room temperature emission be identified as fluorescence from a vibrationally unrelaxed S_1 state (B in Fig. 7). This assignment is not unreasonable since the fluorescent lifetime (14 ps) is within the range of excited state vibrational relaxation times reported for other large aromatic molecules.[18,19] Excitation to a vibrationally "hot" level in S_1 may lead to the establishment of an equilibrium between S_1 and the proton transferred form S_1' prior to vibrational relaxation. The fluorescence decay time would then be determined by the rate of internal conversion, $S_1' \rightsquigarrow S_0'$.[20] If this is the case, the mechanism shown above (eqn. (4)) should be modified to show an equilibrium between S_1 and S_1' and that internal conversion $S_1' \rightsquigarrow S_0'$ occurs prior to vibrational relaxation:

$$S_0 \xrightarrow{h\nu} S_1 \underset{H^+}{\overset{K}{\rightleftharpoons}} S_1' \xrightarrow{ic} S_0' \xrightarrow{H^+} S_0. \qquad (5)$$

The observation of longer fluorescence and ground state recovery lifetimes in ethanol suggests that intermolecular hydrogen bonds with the solvent may inhibit the excited state proton transfer process and/or shift this equilibrium.

Low temperature fluorescence studies in hydrocarbon matrices show an emission maximum at ~625 nm, and lifetimes of ~1 ns at 12K. This emission (R) is assigned to the transition $S_1' \longrightarrow S_0'$ of the proton transferred species shown in Figure 7. The temperature dependence of the fluorescence lifetime is assumed to be wholly due to a temperature dependent nonradiative rate. The activation energy for the temperature dependent nonradiative decay, ~200 cm^{-1}, is of the order of magnitude expected for a torsional vibrational mode. This mode would be expected to be an important factor in the rapid rate of internal conversion in HPB-I.

In the ethanol glass at 12K no highly Stokes shifted emission was observed. The fluorescence maximum occurs at 410 nm, the same region as in the room temperature emission, and in addition, green phosphorescence is observed at 12K. It appears then that in the low temperature ethanol glass, intramolecular proton transfer is slowed and/or the equilibrium shifted to the left in Figure 7, and intersystem crossing becomes a competing nonradiative decay route.

With reference to Figure 7, then, the predominant decay route in the proposed model for relaxation of HPB-I involves uv excitation (double upward arrow) into an excited vibronic level of the molecule that lies at an energy (for 355 nm excitation) above the barrier, if any, between the two excited-state conformations of the molecule. Decay of this vibronic state, at room temperature, is probably controlled by direct internal conversion to the ground state of the tautomeric form of the molecule (S_0'), and not by vibrational relaxation. This internal conversion process is promoted by torsional vibrational modes of the molecule. The rate of this process determines the lifetime of the blue fluorescence (B), and it is slowed in the ethanol solvent due to changes in the excited-state potential surfaces, particularly on the right hand (S_1') side of Figure 7. Ground state recovery of the S_0 state is kinetically controlled in all solvents by both the internal conversion and ground state reverse tautomerization. At low temperatures in solid hydrocarbon matrices the internal conversion rate out of the initially populated level is slowed due to the higher rigidity of the solvent and its effect on the torsional motion of HPB-I. Now vibrational relaxation dominates the decay of this vibronic state, and much stronger red emission (R) is observed. The lifetime of this emission is still controlled, in part, by internal conversion $S_1' \rightsquigarrow S_0'$, however. In alcoholic matrices at low temperature, planar, internally hydrogen-bonded conformations of the molecule are precluded by external hydrogen-bonding, thus preventing proton transfer while simultaneously allowing a competitive intersystem crossing radiationless transition out of S_1.

The model presented above differs from the previously proposed model only in that an equilibrium between vibrationally hot S_1 and S_1' is established and that internal conversion ($S_1' \rightsquigarrow S_0'$) may occur prior to vibrational relaxation. This mechanism may also be applicable to the 2-hydroxybenzophenone class of molecules as well. Since no fluorescence or phosphorescence is observed for HB-I in low temperature hydrocarbon matrices, a very efficient internal conversion process must be occurring in this case.

Other groups have implicated triplet decay pathways for the room temperature nonradiative relaxation of 2-hydroxybenzophenone in ethanol, either because of the presence of two ground state species in solution (intra- and inter-molecularly hydrogen-bonded molecules)[14] or because of only an intermolecularly hydrogen-bonded species with a low excited-state triplet quantum yield.[15] However, there is no compelling reason to invoke the existence of triplet decay routes at room temperature in the case of HB-I molecules. Indeed, we previously suggested[7] that mechanism (4), or the modified form (5), could account for the observations on HB-I in ethanol solution. (The 530-nm absorption kinetics, previously assigned to T-T absorption decay,[15] would have to be reassigned then to tautomeric $S_0' \longrightarrow S_1'$ absorption.[7] Although neither assignment is definite, this latter assignment would yield an $S_0' \rightsquigarrow S_0$ time of ~1.5 ns in HB-I.)

Perhaps differences in the decay behavior of type HB and HPB molecules in hydrocarbon vs. ethanol solvents are due to different solute-solvent interactions in the excited state or ground state tautomer. Interference by ethanol to excited state proton transfer may, however, result in other decay routes becoming available. Triplet formation could then result from a nonproton-transferred species. There is no evidence for triplet formation in room temperature solutions of HPB-I in ethanol suggesting that internal conversion $S_1' \rightsquigarrow S_0'$ is very rapid compared to the rate of intersystem crossing.

Acknowledgment

This research was supported by a contract from the Jet Propulsion Laboratory and, in part, by a grant from the University of California Appropriate Technology Program. We wish to thank Dr. Ami Gupta of J.P.L. for helpful discussions concerning this work. We gratefully acknowledge the work of Ms. Linda DeLucci in typing the manuscript.

References

1. B. Ranby and J. F. Rabek, Photodegradation, Photooxidation and Photostabilization of Polymers: Principles and Applications (Wiley, New York, 1975).
2. H. J. Heller, Europ. Polym. J.-Suppl. p. 105 (1969).
3. A. Gupta, A. Yavrouian, S. diStefano, C. D. Merritt and G. W. Scott, Macromolecules 13, 821 (1980).
4. A. Gupta, M. N. Sarboluki, A. L. Huston, G. W. Scott, W. Pradellok and O. Vogl, Macromolecules, submitted.
5. H. P. Frank and H. Lehner, J. Polymer Sci.: Part C 31, 193 (1970).
6. A. Gupta, G. W. Scott and D. Kliger, in Photodegradation and Photostabilization of Coatings, edited by S. P. Pappas and F. H. Winslow, ACS Symp. Ser. 151, (1980), Chap. 3
7. C. Merritt, G. W. Scott, A. Gupta and A. Yavrouian, Chem. Phys. Letts. 69, 169 (1980).
8. A. L. Huston, C. D. Merritt, G. W. Scott and A. Gupta, in Picosecond Phenomena II, edited by R. M. Hochstrasser, W. Kaiser and C. V. Shank (Springer, Berlin, 1980), p. 232.
9. A. L. Huston, G. W. Scott and A. Gupta, J. Chem. Phys., submitted.
10. A. A. Lamola and L. J. Sharp, J. Phys. Chem. 70, 2634 (1966).
11. R. N. Nurmukhametov, O. I. Detin and D. N. Shigovin, Dokl. Akad. Nauk SSSR 234, 1123 (1977).
12. W. Klopffer, J. Polym. Sci. 57S, 205 (1976); Advan. Photochem. 10, 311 (1977).
13. J. A. Otterstedt, J. Chem. Phys. 58, 5716 (1973).
14. K. J. Choi, L. A. Halliday and M. R. Topp, in Picosecond Phenomena II, edited by R. M. Hochstrasser, W. Kaiser and C. V. Shank (Springer, Berlin, 1980), p. 131.
15. S.-Y. Hou, W. M. Hetherington III, G. M. Korenowski and K. B. Eisenthal, Chem. Phys. Letts. 68, 282 (1979).
16. T. Werner, J. Phys. Chem. 83, 320 (1979).
17. T. Werner, G. Woessner and H. E. A. Kramer, in Photodegradation and Photostabilization of Coatings, edited by S. P. Pappas & F. H. Winslow, ACS Symp. Ser. 151, (1980) Chap. 1.
18. B. I. Greene, R. M. Hochstrasser and R. B. Weisman, Chem. Phys. Letts. 62, 427 (1979).
19. K.-J. Choi and M. R. Topp, Chem. Phys. Letts. 69, 441 (1980).

Excited-State Absorption Spectra and Decay Mechanisms in Organic Photostabilizers [1]

A.L. Huston, C.D. Merritt, and G.W. Scott

Department of Chemistry, University of California,
Riverside, CA 92521, USA

A. Gupta

Energy and Materials Research Section, Jet Propulsion Laboratory,
California Institute of Technology,
Pasadena, CA 91103, USA

14 Springer Series in Chemical Physics
Edited by Fritz Peter Schäfer

Proceedings of the Second International Conference
on Picosecond Phenomena
Cape Cod, Massachusetts, USA
June 18-20, 1980

Editors
R. Hochstrasser W. Kaiser C.V. Shank

Excited-State Absorption Spectra and Decay Mechanisms in Organic Photostabilizers[1]

A.L. Huston, C.D. Merritt, and G.W. Scott

Department of Chemistry, University of California,
Riverside, CA 92521, USA

A. Gupta

Energy and Materials Research Section, Jet Propulsion Laboratory,
California Institute of Technology,
Pasadena, CA 91103, USA

1. Introduction

This paper discusses picosecond spectroscopic studies of excited-state decay mechanisms in widely-used, ultraviolet-absorbing, polymer photostabilizers—2-hydroxybenzophenone (I) and 2-(2'-hydroxy-5'-methylphenyl)-benzotriazole (II)—the structures of which are shown below:

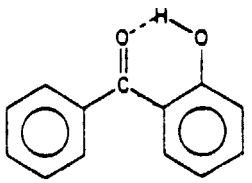

(I)

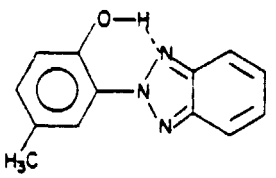

(II)

An intramolecular hydrogen bond in these molecules is thought to promote rapid excited-state internal proton transfer and subsequent excited-state decay. However, the detailed mechanism and kinetics of these processes have not been determined. Related studies on organic photostabilizers have been reported for salicylates [1,2], 2-(2'-hydroxyphenyl)-s-triazines [3], and 2-hydroxybenzophenones [4-6].

2. Experimental

Excitation of (I), (II), and a derivative of (II) was accomplished with a third-harmonic pulse ($\Delta t \approx 8$ ps, λ=355 nm) from a modelocked Nd^{+3}:glass laser system. Excited state absorption spectra were obtained as previously described [5] by probing the excited sample with a time-delayed continuum pulse and recording a single-shot, double-beam-corrected spectrum (400-700 nm) with a spectrograph and an optical multichannel analyzer (EG&G PARC, OMA 2). Excited-state absorption kinetics were obtained using a delayed probe pulse from a short-cavity dye laser as previously described [7]. Absorption bleaching-recovery kinetics at 355 nm were also obtained with attenuated third-harmonic probe pulses.

[1]This research was supported by the ASTT project of Solar Thermal Power Systems of the Jet Propulsion Laboratory. Partial support by the California Institute of Technology President's Fund and the Committee on Research at the University of California, Riverside, is also acknowledged.

3. Results and Discussion

3.1. 2-hydroxybenzophenone

Excited-state absorption spectra of 2-hydroxybenzophenone (I), obtained at three delay times in several solvents, are summarized in the Table. These spectra are quite broad and weak. The maximum O.D. change observed [illegible] 13. Under identical experimental conditions, a T-T absorption [illegible] benzophenone in ethanol has a maximum O.D. of 0.6 at ~530 nm.

Table Summary of observed transient absorption spectra

Molecule	Solvent	Delay Time [ps]	λ_{max} [nm]	O.D.@λ_{max}
2-hydroxybenzophenone (I)	CH_2Cl_2	7	435	0.10
		20	450(v.broad)	<0.04
		485	---	<0.03
	isooctane	7	450	<0.04
		20	---	<0.03
		485	---	<0.03
	cis-1,3-pentadiene	7	450(v.broad)	0.05
		20	---	<0.03
	ethanol	7	435	0.08
		17	<400;475	>0.10;0.09
		50	420	0.13
		480	450	0.07
2-(2'-hydroxy-5'-methylphenyl) benzotriazole (II)	CH_2Cl_2	7	440	0.11
		20	---	<0.03
		485	460	0.10
	ethanol	7	435;500	0.07;0.07
		20	440	<0.04
		485	460	0.10
2-(2'-acetoxy-5'-methylphenyl) benzotriazole (acetoxy-II)	CH_2Cl_2	7	470	0.37
		20	475	0.42
		485	465	0.21

There has been some controversy regarding the decay mechanism of (I). KLÖPFFER [8] has proposed that the main decay route occurs via the triplet mainfold following proton transfer in the singlet state. In nonhydrogen-bonding solvents, however, no long-time absorption (i.e., T_n~T_1) is observed in our experiments indicating that few of the excited singlet state molecules of (I) intersystem cross to the triplet. (See the Table; the experiment in cis-1,3-pentadiene confirms that the short-time absorption is probably due to a singlet.) In ethanol, some visible absorption remains at "long" time (480 ps) and thus some of the molecules of (I) may intersystem cross in hydrogen-bonding solvents. This interpretation is consistent with other recent studies [4] and with previously reported [10] quantum yields of quenchable triplets of (I) in nonhydrogen-bonding and hydrogen-bonding solvents (Φ_T=0.03 in cyclohexane and Φ_T=0.15 in ethanol).

3.2. 2-(2'-hydroxy-5'-methylphenyl)benzotriazole

Excited-state absorption spectra of 2-(2'-hydroxy-5'-methylphenyl)benzotriazole (II) and 2-(2'-acetoxy-5'-methylphenyl)benzotriazole (acetoxy-II) in methylene chloride are shown in Figs. 1A and 1B, respectively. These and similar spectra of (II) in ethanol are summarized in the Table above.

For (II) in both solvents, absorption at 7 ps in the blue decays to within the noise level by 20 ps. At longer time (485 ps), a different absorption in the blue appears. Our tentative interpretation of these spectra follows the decay mechanism suggested by WERNER [10]:

$$S_0 \xrightarrow{h\nu} S_1 \xrightarrow[k_1]{H^+ \text{ trans.}} S_1' \xrightarrow[k_2]{\text{i.c.}} S_0' \xrightarrow[k_3]{H^+ \text{ trans.}} S_0 \quad , \qquad (1)$$

in which a prime designates proton transfer from oxygen to a nitrogen. Thus at 7 ps, we assign the observed spectrum of (II) to $S_n \rightarrow S_1$ based on similar spectra of acetoxy-II) shown above. By 20 ps, rapid proton transfer has occured, yielding a weak, essentially featureless $S_n' \rightarrow S_1'$ spectrum in the visible. By 485 ps, internal conversion to the ground state of the proton-transferred species has occurred, yielding the $S_1' \rightarrow S_0'$ spectrum. In support of this last assignment, the absorption spectrum observed at 485 ps is the approximate mirror image of previously reported $S_1' \rightarrow S_0'$ fluorescence [10,11]. This interpretation suggests that there may be a barrier (of unknown height) to proton back-transfer in the ground state. It has been estimated [10] that the proton is favored to be on oxygen by $\Delta H = 16$ kcal/mole in the ground state.

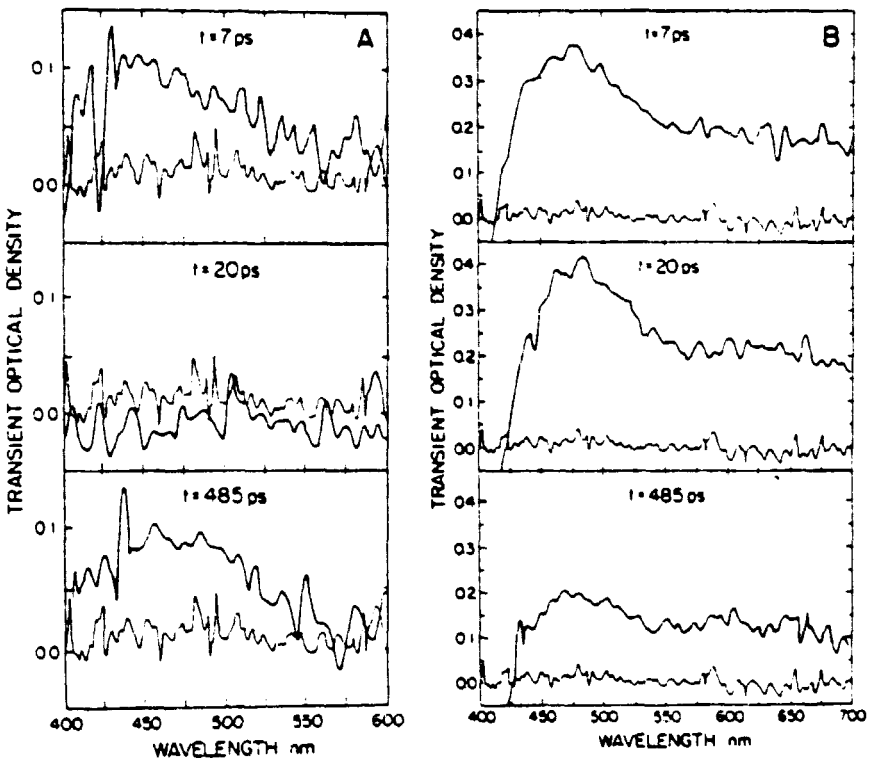

Fig. 1 Transient absorption spectra of (II) in CH_2Cl_2 (A) and of (acetoxy-II) in CH_2Cl_2 (B) at selected delay times

In (acetoxy-II), chemical modification precludes proton transfer. The observed spectra (Fig. 1B) are assigned to mostly $S_n \leftarrow S_1$ absorption. The absorption decay in (acetoxy-II) at 455 nm following excitation at 355 nm (Fig. 2) is consistent with exponential decay to a nonzero asymptote. The least squares fit rate constant is $(3.9\pm0.5)\times10^9$ sec^{-1} (τ_{S_1}=0.26 ns). The long-

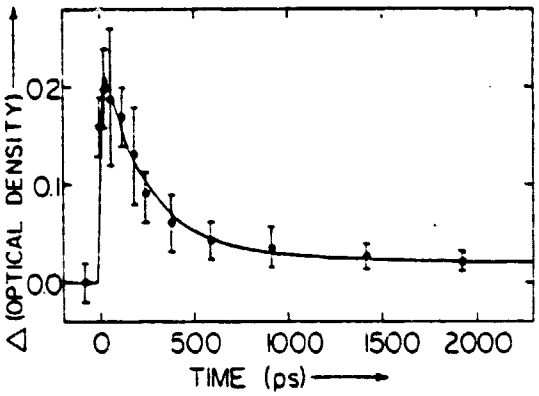

Fig. 2 Kinetics of optical density changes of (acetoxy-II) in CH_2Cl_2 at 455 nm

time, asymptotic absorption is assigned to $T_n \leftarrow T_1$ absorption. In a nanosecond flash photolysis experiment, $T_n \leftarrow T_1$ absorption peaking at ~425 nm decays with an ~200 ns lifetime [12]. We determined the triplet quantum yield of (acetoxy-II) to be ϕ_T>0.3. Thus the S_1 lifetime of (acetoxy-II) is at least partially controlled by intersystem crossing.

Absorption bleaching-recovery kinetics at 355 nm were obtained for (II) in both ethanol and methylene chloride. The result in the methylene chloride solvent is shown in Fig. 3. In this experiment the ground state optical density of the sample was arranged to be ~0.6 at 355 nm, and the excitation and probe pulses had parallel linear polarization. The changes in optical density plotted in Fig. 3 correspond to decreases in optical density at 355 nm. In ethanol, a qualitatively similar result is obtained. The unusual behavior between 0 and 100 ps is in qualitative agreement with (1). That is, at 355 nm, S_1 absorbs less strongly than S_0; S_1 rapidly decays by proton transfer to S_1' (in <50 ps), a state which absorbs more strongly than the ground state; S_1' internally converts to S_0' (in ~100 ps after excitation), a state which absorbs less strongly than S_1'; and S_0' then decays more slowly to S_0. Although the data do not uniquely determine the rates of these processes, the smooth curve in Fig. 3 was obtained using k_1=15ns^{-1}, k_2=50ns^{-1}, and k_3=5ns^{-1} by convoluting rate expressions derived from (1) with the laser pulse durations.

Eq. (1) is not the only mechanism which can qualitatively reproduce the observed kinetics in Fig. 3. However, if one is restricted to a sequential decay mechanism like (1), then to obtain even qualitative agreement with the data, requires that $k_2 \geq k_1$=10-20 ns$^{-1} > k_3$. Furthermore, the extinction coefficients at 355 nm of the states involved must be ordered $\epsilon(S_1') > \epsilon(S_0) > \epsilon(S_1) > \epsilon(S_0')$, and at least three intermediates are involved. The values of the rate constants and extinction coefficients are not uniquely determined by the

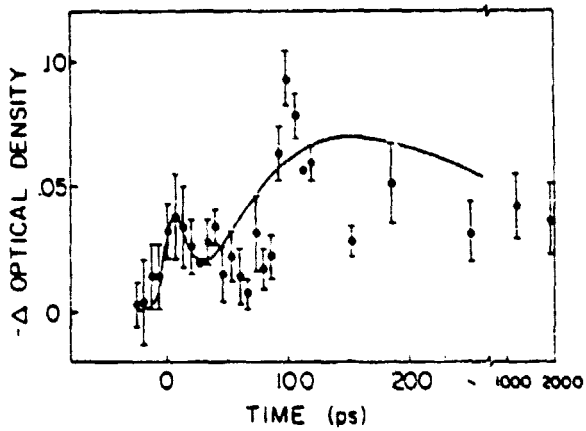

Fig. 3 Kinetics of optical density changes of (II) in CH_2Cl_2 at 355 nm.

data. Reorientation of the transition dipoles of the various states was not included in the kinetics model used to obtain the curve in Fig. 3.

We have also investigated the emission kinetics of solutions of (II) in ethanol and methylene chloride at room temperature, exciting with a 7-ns uv-pulse from a nitrogen laser. In both cases, prompt emission which followed the laser excitation pulse within the time resolution of the detection system (~0.5 ns) was observed. Thus, this emission, centered at ~420-450 nm, necessarily has a lifetime of <1 ns. Based on these observations, this emission is assigned to $S_1 \rightarrow S_0$ and is consistent with our other observations on (II).

References

[1] K.K. Smith and K.J. Kaufmann, J. Phys. Chem. 82, 2286 (1979); and in A.H. Zewail (ed.), *Advances in Laser Chemistry*, Springer Series in Chemical Physics, Vol. 3 (Springer, Berlin, Heidelberg, New York 1978) 163
[2] P.J. Thistlethwaite and G.J. Woolfe, Chem. Phys. Letts. 63, 401 (1979).
[3] H. Shizuka, K. Matsui, Y. Hirata, and I. Tanaka, J. Phys. Chem. 80, 2070 (1976); 81, 2243 (1977).
[4] S.-Y. Hou, W.M. Hetherington III, G.M. Korenowski, and K. B. Eisenthal, Chem. Phys. Letts. 68, 282 (1979).
[5] C. Merritt, G.W. Scott, A. Gupta, and A. Yavrouian, Chem. Phys. Letts. 69, 169 (1980)
[6] M.R. Topp, unpublished results.
[7] R.W. Anderson, Jr., D.E. Damschen, G.W. Scott, and L.D. Talley, J. Chem. Phys. 71, 1134 (1979).
[8] W. Klöpffer, J. Polym. Sci: Symp. 57, 205 (1976); Adv. in Photochem. 10, 311 (1977).
[9] A.A. Lamola and L.J. Sharp, J. Phys. Chem. 70, 2634 (1966).
[10] T. Werner, J. Phys. Chem. 83, 320 (1979).
[11] J.-E.A. Otterstedt, J. Chem. Phys. 58, 5716 (1973).
[12] A. Gupta, D.S. Kliger, and R. Liang, unpublished results.